Circulation
Cardiovascular Genetics
JOURNAL OF THE AMERICAN HEART ASSOCIATION

American Heart Association
Learn and Live

Comparative LipidomicS Profiling of Human Atherosclerotic Plaques

Christin Stegemann, Ignat Drozdov, Joseph Shalhoub, Julia Humphries, Christophe Ladroue, Athanasios Didangelos, Mark Baumert, Mark Allen, Alun H. Davies, Claudia Monaco, Alberto Smith, Qingbo Xu and Manuel Mayr

Circ Cardiovasc Genet published online April 21, 2011;
DOI: 10.1161/CIRCGENETICS.110.959098
Circulation: Cardiovascular Genetics is published by the American Heart Association. 7272 Greenville Avenue, Dallas, TX 72514
 Print ISSN: 1942-325X. Online ISSN: 1942-3268

Comparative LipidomicS Profiling of Human Atherosclerotic Plaques

Running title: *Stegemann et al.; Lipidomics of atherosclerotic plaques*

Christin Stegemann, PhD[1]; Ignat Drozdov, MSc[1]; Joseph Shalhoub, BSc, MBBS, MRCS[2]; Julia Humphries, PhD[1]; Christophe Ladroue, PhD[3]; Athanasios Didangelos, PhD[1]; Mark Baumert, BSc[4]; Mark Allen, PhD[4]; Alun H Davies, MA, DM, FRCS, FHEA[5]; Claudia Monaco, MD, PhD[2]; Alberto Smith, PhD[1]; Qingbo Xu, MD, PhD[1]; Manuel Mayr, MD, PhD[1]

[1]King's British Heart Foundation Centre, King's College London; [2]Kennedy Institute, Imperial College London; [3]University of Warwick, Warwick; [4]Advion Biosciences, Ltd., Norwich; [5]Imperial College, Vascular Unit, London, United Kingdom

Correspondence:

Prof. Manuel Mayr

King's British Heart Foundation Centre

King's College London

125 Coldharbour Lane, London SE5 9NU

United Kingdom

Tel number: +44 (0)20 7848 5132

Fax number: +44 (0)20 7848 5296

E-mail: manuel.mayr@kcl.ac.uk

Journal Subject Codes: [76] Carotid endarterectomy; [134] Pathophysiology; [144] Other arteriosclerosis; [90] Lipid and lipoprotein metabolism; [97] Other Vascular biology

Abstract:

Background - We sought to perform a systematic lipid analysis of atherosclerotic plaques using emerging mass spectrometry techniques.

Methods and Results – A chip-based robotic nanoelectrospray platform interfaced to a triple quadrupole mass spectrometer was adapted to analyse lipids in tissue sections as well as extracts from human endarterectomy specimens by shotgun lipidomics. 18 scans for different lipid classes plus additional ones for fatty acids resulted in the detection of 150 lipid species from 9 different classes, of which 24 were detected in endarterectomies only. Further analyses focused on plaques from symptomatic and asymptomatic patients and stable versus unstable regions within the same lesion. Polyunsaturated cholesteryl esters with long chain fatty acids and certain sphingomyelin species showed the greatest relative enrichment in plaques compared to plasma and formed part of a lipid signature for vulnerable and stable plaque areas in a systems-wide network analysis. In principal component analyses the combination of lipid species across different classes provided a better separation of stable and unstable areas than individual lipid classes.

Conclusions - This comprehensive analysis of plaque lipids demonstrates the potential of lipidomics for unravelling the lipid heterogeneity within atherosclerotic lesions.

Key words: atherosclerosis, carotid endarterectomy, mass spectrometry, lipids, metabolomics

According to the response-to-retention hypothesis, the binding of cholesterol-containing lipoprotein particles to intimal proteoglycans is the central pathogenic process in atherogenesis.[1] Once retained, lipoproteins get oxidized, accumulate in "foam cells“ and provoke a cascade of inflammatory processes, which drive the formation of atherosclerosis and ultimately define the propensity of the plaque to rupture. In most studies, the lipid content in plaques is just visualized by oil red O staining. A more detailed characterization, including the detection of single lipid species rather than lipid classes, may provide a better classification of atherosclerotic lesions with the goal of illuminating biology and discovering clinical biomarkers.[2,3]

Although the potential of mass spectrometry (MS) has long been recognized[4], it is the recent progress in MS technologies that has transformed our ability to profile atherosclerotic plaques by allowing the quantitation of hundreds of individual lipid species in complex biological samples.[5,6] For example, a recent study demonstrated that lipids in murine lesions can be imaged by multiplex coherent anti-stokes Raman spectroscopy.[3] Another study applied desorption electrospray ionization MS (DESI-MS) to image and identify 26 distinct lipid species in a single human plaque.[7] A MS-based analysis comparing different human atherosclerotic lesions has not been reported to date. To reveal a characteristic lipid signature for plaque vulnerability, we took advantage of the latest MS developments in shotgun lipidomics and compared radial arteries, endarterectomy samples from symptomatic and asymptomatic patients as well as stable and unstable areas within the same symptomatic lesion.

METHODS

Clinical samples. The study was approved by the Research Ethics Committees of King’s College London and Imperial College London. All patients gave their written informed consent. Surgical samples were derived from carotid or femoral endarterectomies and radial arteries. In total, 26 patients were included in this study. Their clinical characteristics are provided in the Online Supplement. Control radial arteries were carefully chosen to ensure they were free of macroscopically evident vascular pathology, including atherosclerosis. Samples were briefly rinsed with cold PBS to remove superficial blood, snap-frozen in liquid nitrogen and stored at -80°C (average storage time: 3.4 ± 1.4 years). Eight carotid plaques from symptomatic patients were dissected into ruptured versus non-ruptured areas before freezing.

Liquid extraction surface analysis (LESA) coupled to nano-ESI-MS. Frozen human plaques were cut at 200 µm using a rotary microtome (Microm HM560 cryostat, Thermo Scientific), placed on electrostatically charged slides (Superfrost Plus, BDH) and air dried for 15–30 min. Lipids were directly analyzed from tissue sections with a Advion TriVersa NanoMate system (Advion BioSciences Inc., Ithaca, NY) controlled by Chipsoft software (v8.1.0.928, Advion BioSciences) coupled to a triple quadrupole mass spectrometer (QqQ-MS, TSQ Vantage, Thermo Fisher Scientific, UK). The solvent extraction volume was 1.5 µL (chloroform/methanol/isopropanol 1:2:4 containing 7.5 mM ammonium acetate) and the dispensed volume was 1.0 µL. Solvents were sprayed through a 4.1-µm nozzle diameter chip (Advion BioSciences) at an ionization voltage of 1.2 kV and a gas pressure of 0.3 psi. The first and third quadrupoles (mass resolution 0.7 Th) served as independent mass analyzers while the second quadrupole was used as collision cell (argon was used as collision gas with a pressure of 1.0 mTorr) for tandem mass spectrometry. The temperature of the ion transfer capillary was maintained at 150 °C. Full MS spectra and precursor ion scans (PI) for CEs (PI 369.3) and PCs (PI 184.1) from different plaque sections were acquired over a period of 6 min.

Lipid extraction. Lipids were extracted from endarterectomies and control radial arteries (> 25 mg wet weight) using an adaptation of the Folch method.[8] A detailed description is available in the Online Supplement. Plasma samples were obtained from 35 patients undergoing carotid endarterectomy. 10 μL of plasma was used for lipid extraction using an adaption of a recently published method.[9] Details are included online.

Shotgun lipidomics. Aliquots from tissue extracts were reconstituted in 500 μl chloroform/methanol 1:2 and further diluted 1:100 with chloroform/methanol/isopropanol 1:2:4 containing 7.5 mM ammonium acetate. Plasma extracts were diluted 1:10 with chloroform/methanol/isopropanol 1:2:4 containing 7.5 mM ammonium for MS analysis. Just prior to analysis, samples were centrifuged at 12,000 rpm for 2 min and analyzed with a TriVersa NanoMate coupled to a QqQ-MS as described above. An ionization voltage of 0.95 – 1.40 and a gas pressure of 1.25 psi was used.[10] Full MS spectra were acquired over a 1 min period of signal averaging in the profile mode in both positive and negative mode. The intensity of the full MS in positive mode was one magnitude higher than the one in negative ion mode. For NL and PI scans the collision gas pressure (argon) was set at 1.0 mTorr, the collision energy was chosen depending on the classes of lipids. Spectra were automatically acquired with rolling scan events by a sequence subroutine operated under the Xcalibur software (Thermo, version 2.0.7). The different neutral loss and precursor ion scans were set according to Brugger *et al*.[11] or Han and Gross[12,13] (**Supplemental Table I**). The main classes of lipids in positive ion mode were phosphatidylethanolamine (PE)/lysoPE (lPE), phosphatidylserine (PS)/lyso PS (lPS), cholesteryl ester (CE), triacylglycerol (TAG), phosphatidylcholine (PC)/lyso-PC (lPC) and sphingomyelin (SM). The PI scan of the acetate ion of the most abundant PC species in the negative ion mode was used for the identification of PC-derived fatty acids. The same parent ion scan at 184.1 was used for the identification of SMs, but the nitrogen rule allowed a discrimination of these two lipid classes. SMs with two nitrogen atoms appear at odd m/z values, whereas PC-signals occur at even m/z values.[11] To further separate PCs from SMs, SMs were identified in negative ion mode by precursor ion scan at m/z 168.0[11] (**Supplemental Figure I**). For lipid quantification, 392 pmol of CE 19:0 (Avanti polar lipids, Alabaster, AL) was added to 100 µL of each sample as internal standard and analyzed for 2 min using a PI scan at m/z 369.3. The coefficient of variation for these measurements was <10% in 58% (53%) of the analytes, 10% to 20% in 18% (28%) of the analytes, 20% to 40% in 5% (5%) of the analytes, and >40% in the remainder for intraday (interday) measurements. For quantification of PC, lPC and SM species 52 pmol PC(17:0/17:0), 46.4 pmol/µL lPC(19:0), and 61.2 pmol SM(d18:1/12:0) were added per 100 µL sample (all Avanti polar lipids) and analyzed for 2 min using a PI scan at 184.1.

Data processing. QqQ-MS data were analyzed with Xcalibur (version 2.0.7, ThermoFisher, USA). Lipid identifications were based on their characteristic head groups and corresponding fatty acids or using the LipidMaps database and Lipid MS Predictor (v1.5) available at http://www.lipidmaps.org. For quantitation, a peak list was generated and imported into LIMSA software (version 1.0)[14] using the following settings: linear fit, offset = 0, peak fwhm = 0.5, sensitivity = 0.1.

Nomenclature. We followed the designations and abbreviations recommended by IUPAC (http://www.chem.qmul.ac.uk/iupac/lipid). Glycero- and glycerophospholipids were named with shorthand notification and numbers separated by colons refer to carbon chain length and number of double bonds. The composition of the side chains for the glycero- and glycerophospholipids were not assigned and were used randomly for glycerolipids. For glycerophospholipids, the unsaturated fatty acid was set on *sn*-1 position and the saturated on *sn*-2. Sphingolipids are presented in the order of long-chain base and *N*-acyl substituent.

Statistical analysis. Statistical analysis was performed using the Student's t-test or analysis of variance and Scheffe's post hoc test. A p value of <0.05 was considered significant. Principal component analysis (PCA) were performed in Matlab (2009a, The Mathworks Limited). Capacity of each lipid to differentiate plaque or plasma samples was assessed using the out-of-bag estimates of feature importance provided by the *TreeBagger* class for Matlab. Data were normalized by expressing individual lipid intensities as percentage of accumulative intensities in each lipid class.

RESULTS

Workflow overview. Using a triple quadrupole mass spectrometer (QqQ-MS), two different approaches were compared (**Figure 1A**): *1)* Liquid extraction surface analysis (LESA) for direct extraction of plaque lipids from tissue sections[15,16] and *2)* Shotgun lipidomics as described by Han and Gross[12] for the analysis of tissue extracts. First a full MS scan in positive and negative ion mode was acquired. Then, product ion (PI) and neutral loss (NL) scans, characteristic for different lipid classes, unambiguously identified certain lipids by their characteristic MS/MS product ions (see example for CE identification, **Figure 1B**).

LESA versus tissue extracts. For LESA, frozen human carotid endarterectomy samples were cut into thin sections without optimal cutting temperature (OCT) compound to avoid a contamination with polyethylene glycol. 1.5 µL extraction solution was sufficient to provide a stable spray for over 10 min. The signals within the lipid relevant m/z range of 400 – 1000 in the full MS scan (**Figure 2A**) were comparable to the ones obtained by shotgun lipidomics from tissue extracts (**Figure 2B**). Also, the lipid class specific head group scans (see **Figure 2 C, D** for PI 184.1 for lPC, PC and SMs and **Figure 2E, F** for PI 369.3 for CEs) showed similar peaks and signal intensities (see **Figure 2C, E** for tissue sections; **Figure 2D, F** for tissue extracts). Notably, lPC species within the m/z range of 490 – 540 were detected in tissue sections as well as tissue extracts, confirming that these degradation products are present in human atherosclerotic plaques and not artifacts of the extraction procedure.

Identification of plaque-lipids. A comparative lipid analysis of radial arteries, carotid and femoral endarterectomies was performed. The patients' clinical characteristics are provided in **Supplemental Table II**. 6 scans in positive ion mode and 14 in negative ion mode resulted in the identification of 150 different lipid species (**Supplemental Table III and IV**), of which 24 were detected in atherosclerotic plaques only (**Table 1**). TAGs accounted for the few prominent signals between m/z 790 and 930 in the full MS of radial arteries (**C1 – C3, Figure 3A**). In contrast, the full MS scan of endarterectomy samples was dominated by CE, SM, PC and TAG species (**P1 – P3, Figure 3A**). Scans for specific lipid head groups detected lPCs, PCs, lPEs, PEs, lPSs, SMs, CEs and TAGs. Unlike previous studies in human aortas,[17,18] PS species were also identified. Scans for acylcarnitine, phosphatidylinositol, phosphatidylinositol-phosphates, phosphatidylinositol (4,5) bisphosphate, sulfatides, acylCoA, ceramides and cerebrosides did not reveal strong enough signals for these lipid classes in shotgun lipidomics.

Quantitation of plaque-lipids. A comparison between control arteries and endarterectomies revealed that the signal intensities of the head group scans for lPCs, PCs and SMs differed by one and for CE by two orders of magnitude (**Figure 3B)**. To calculate the total amount of CEs, lPCs, PCs and SMs in atherosclerotic plaques, authentic standards were spiked into the samples. The highest accumulation was observed for CE species (**Table 2**). The average CE content was 23.9 mg/g in plaques compared to 0.2 mg/g in control arteries (**Figure 4A**). As expected, oleic (18:1) and linoleic acid (18:2) were the most common fatty acids (**Supplemental Table V**). The relative distribution of CEs identified in plaque and control arteries is depicted in **Figure 4B**.

Comparison of carotid endarterectomies. Next, we compared the lipid content of carotid endarterectomy samples from closely matched symptomatic and asymptomatic patients (n=6 per group). Their clinical characteristics are provided in **Supplemental**

Table VI. PCA was performed to investigate the global variation of the patient samples in their lipid profiles. The distance between symptomatic and asymptomatic patients in PCA was negligible although the two first principal components captured 97% of the variance (**Supplemental Figure II**). Given the heterogeneity of carotid endarterectomy samples, plaques excised from symptomatic and asymptomatic patients may share similar features. To reduce heterogeneity, in another cohort of patients (**Supplemental Table VII**), the stable area of the plaque with no signs of rupture was carefully separated from the unstable area, in which there was 'ulceration' of the surface with or without thrombosis and/or intraplaque haemorrhage, thereby providing an internal control for each sample and minimizing interpatient variability. Quantitative data for all lipid measurements in stable and unstable plaque areas are included as **Supplemental Table VIII.** The 10 most differentially expressed species from 4 different lipid classes were sufficient to separate stable and unstable areas within the same lesion in PCA (**Figure 5**). No separation was obtained with individual lipid classes (**Figure 5**).

Comparison to plasma lipids. Plasma samples of 35 patients undergoing carotid endarterectomies were analyzed by shotgun lipidomics. Their clinical characteristics are provided in **Supplemental Table IX.** Compared to recent studies on plasma lipids using either direct injection[10] or ultra performance LC-MS,[9,19] twice as many CE species were detected by our shotgun approach. In total, 10 CEs, 9 SMs, 8 lPCs and 31 PCs were identified (**Supplemental Table X**). As expected, plaque and plasma samples were well separated by PCA (**Figure 6A)**. The main lipids contributing to this separation were CE, PC and SM species (**Figure 6B**). The quantitative values of the different species and their relative distribution are provided in **Supplemental Figures III-VI**. In agreement with previous reports,[20] CE18:2 constituted approximately 40% of all CE species in plasma from patients with endarterectomies, but accounted for only 28% in plaques. In contrast, the relative contribution of CE18:1 to the total CE content was similar in plaques and plasma (about 30%). Polyunsaturated CE with long chain fatty acids, which were previously undetectable in plasma by thin layer chromatography,[20] showed the strongest relative enrichment in plaques among all CE species analysed (**Table 3 and Figure 6A**). Their relative contribution to the total CE content declined in ruptured (unstable) compared to stable regions, i.e. CE20:3 (P value < 0.006).

Systems-wide analysis of plaque lipids. Lipid expression similarity in plaques from asymptomatic and symptomatic patients as well as in stable and unstable areas within the same lesion was inferred using Pearson Correlation Coefficients (PCC) and visualized as networks where nodes correspond to lipids and edges link correlated pairs (PCC≥0.70). Clusters of interlinked lipids were identified using an unbiased network clustering algorithm.[21] This systems-wide analysis revealed plaque-specific lipid signatures consisting of 19 lipid species in asymptomatic-symptomatic lesions (**Figure 7A**), 12 lipid species in stable-unstable plaque areas (**Figure 7B**), and 33 common lipid species that were differentially linked in the two networks (**Figure 7A**, **B**). Unbiased network clustering[21] demonstrated that lipid species belonging to the same class were more likely to be linked in the stable-unstable network of different areas within the same lesions (e.g CE22:4, CE22:5, and CE22:6). These connectivity patterns were not observed in the asymptomatic-symptomatic network comparing plaques from different patients. Thus, the lipid composition as well as the connectivity between lipid species may contribute towards a better characterization of atherosclerotic lesions.

DISCUSSION

While lipids of human atherosclerotic plaques have previously been analyzed, target-focused measurements restricted to individual lipid classes remain insufficient to reveal the global lipid imbalances in atherosclerosis. This study demonstrates the integration of advanced MS toward a better characterization of the lipid composition in atherosclerosis.

QqQ-MS. The different scan options of the QqQ-MS can resolve isobaric lipids from different lipid subclasses and detect less prominent species in the presence of high abundant lipids. Notably, LESA allowed a rapid analysis of plaque lipids directly from tissue sections without time and labor-intensive sample preparation. To the best of our knowledge this is the first time that LESA was used in combination with a QqQ-MS for lipid profiling. The signals as well as the signal intensities were comparable to shotgun lipidomics of tissue extracts (**Figure 2**). For quantification, lipid extracts were spiked with class specific internal standards. Since specificity is achieved by the characteristic headgroup scans on the QqQ-MS, only a single standard per lipid class is required. Thus, the shotgun lipidomics approach is less expensive compared to other MS-based lipid analysis techniques and applicable to tissue sections as well as extracts.

Lipids in atherosclerosis. Cholesterol within the vasculature accumulates as CE, either as a droplet in the cytosol or in lysosomes.[22] Infiltrating LDL-particles contain a CE-rich core with linoleic acid (18:2) as the most abundant polyunsaturated fatty acid.[23] The intimate relationship of plasma lipids, vascular matrix and CE deposits in the arterial wall is well documented.[24-26] Currently, our knowledge at the biological level is mostly related to the classes of lipids rather than the bioactivity of single lipid species within these classes.[2] Yet, the actual species composition of the lipid classes is likely to be an important atherogenic factor, i.e. LDL particles enriched with monounsaturated cholesteryl oleate (CE18:1) are typically larger and more active in binding to arterial proteoglycans, thereby favoring retention and subsequent formation of early atherosclerotic lesions.[27] In comparison, LDL particles enriched with polyunsaturated cholesteryl linoleate (CE18:2) are thought to be less atherogenic.

Shotgun lipidomics of plaques. In total, 150 lipid species were identified in plaques. The lipid classes accounting for the major differences between control and diseased arteries were CEs, SMs, lPCs and PCs. Remarkabl differences were observed for the relative amount of CEs with linoleic acid and polyunsaturated fatty acids like arachidonic acid (**Figure 4**), substrates for inflammatory mediators and mediators of resolution. The observed decrease in polyunsaturated fatty acids coupled with an increase in linoleic acid in human plaques could be an indicator for reduced production of mediators for inflammatory resolution (lipoxins, resolvins and protectins).[28] A simple, rapid macroscopic method of classification based on the definitions of plaque progression and instability by Stary et al.,[29] was used to differentiate ruptured (unstable) versus non-ruptured (stable) segments of the same plaque (**Figure 5**).[30,31] In this comparison, where each patient serves as its own control, the lipidomics approach was most successful and provided insights in the lipid heterogeneity within atherosclerotic plaques. Consistent with previous reports,[20] CE(18:2) was the major CE species in atherosclerosis and the relative distribution of most CEs was comparable to results obtained by thin layer chromatography, providing independent validation of the quantitative accuracy of our approach. The sensitivity of shotgun lipidomics, however, allowed the identification of additional CE species as well as other lipid classes, such as lPCs (a by-product of LDL oxidation and formed by the enzymes phospholipase A_1, phospholipase A_2 or lecithin:cholesterol acyltransferase) and SMs (an ubiquitous component of cell membranes and of the LDL surface). Plasma lipoproteins are the main source for SMs[18] and high SM plasma levels were associated with coronary artery disease.[32] SM and its hydrolyzing enzyme sphingomyelinase (SMase) are believed to mediate biological effects, but the mechanistic links between SM and atherosclerosis remain elusive.[33] SMs with long chain fatty acids were substantially lower in plaques compared to plasma whereas certain SM species, i.e. SM(d18:1/16:0) and SM(d18:1/14:0), were enriched supporting the hypothesis that there are either selectively retained or *de novo* synthesized in atherosclerotic plaques.[34] Similarly, the enrichment of lPCs[35] is supposed to contribute to the pathogenesis of atherosclerosis and in particular inflammation.[36]

Systems-wide network analysis. The post-genomic shift in paradigm from reductionism to systems-wide network inference acknowledges the fact that biological systems are pleiotropic and interconnected.[37] Similarly, systemic relationships between lipid classes in atherosclerotic lesions are important for understanding genotype-phenotype relationships[38] and working towards a lipid signature for risk prediction, early diagnosis, and personalized treatment of this disease. Previous studies enabled only a partial analysis of plaque lipids and mainly focused on LDL,[24,39-41] cholesterol and its derivatives.[41,42] There are also publications about individual lipid classes in atherosclerotic plaques, i.e. on isoprostanes,[23] lipid mediators,[4] lPCs,[35] oxidized PCs,[43] and phospholipids[44] but no comprehensive comparison between control and diseased arteries across different lipid classes has been performed to date. Manicke et al. recently applied DESI-MS to atherosclerotic plaque tissue.[7] As proof-of-principle, lipid profiling was performed on a single human plaque in positive and negative ion mode and 26 lipid species were identified. Our shotgun lipidomic approach identified all of the 26 lipids except SM 22:0 (**Supplemental Table III** and **IV**). Moreover, we were able to show that 16 out of the 26 lipids in the former study were present in control arteries and are therefore not plaque-specific. Using a network approach, we demonstrate that homogeneous lipid clusters were identified in the stable-unstable network from the same lesion (**Figure 7**) and that sampling differentially expressed species across lipid classes improves the separation in PCA (**Figure 5**).

Limitations of the study. While MS has proven a valuable tool for comparative lipid analysis, minor components like signaling molecules (sphingosine-1-phosphate[45] or isoprostanes) or oxidized lipids remain undetected. Chromatographic separation would be essential to analyze these scarce lipid species. Also, modified lipids with alterations in the characteristic head groups as well as free cholesterol and other species, which do not readily ionize by ESI, are not detected in our analysis. Finally, LESA only provides a qualitative comparison of plaque lipids as lipid extracts have to be spiked with authentic standards for quantitation.

Conclusions. To our knowledge, this study is the most comprehensive MS analysis of the lipid content in human atherosclerotic plaque to date. An in-depth comparison of the lipid composition in different atherosclerotic lesions combined with systems-wide network analysis unraveled plaque-specific lipid signatures. In future, these advanced technologies could be exploited for diagnostic purposes or as a platform for drug screening.

Funding Sources: This work was supported by grants from the British Heart Foundation and Oak Foundation. M.M. is a Senior Research Fellow of the British Heart Foundation.

Conflict of Interest Disclosures. None.

References:

1. Williams KJ, Tabas I. The response-to-retention hypothesis of early atherogenesis. Arterioscler Thromb Vasc Biol. 1995;15:551-561.
2. Hu C, van der Heijden R., Wang M, van der Greef J., Hankemeier T, Xu G. Analytical strategies in lipidomics and applications in disease biomarker discovery. J Chromatogr B Analyt Technol Biomed Life Sci. 2009;877:2836-2846.
3. Kim SH, Lee ES, Lee JY, Lee ES, Lee BS, Park JE, Moon DW. Multiplex coherent anti-stokes Raman spectroscopy images intact atheromatous lesions and concomitantly

identifies distinct chemical profiles of atherosclerotic lipids. Circ Res. 2010;106:1332-1341.

4. Brezinski DA, Nesto RW, Serhan CN. Angioplasty triggers intracoronary leukotrienes and lipoxin A4. Impact of aspirin therapy. Circulation. 1992;86:56-63.

5. Gerszten RE, Wang TJ. The search for new cardiovascular biomarkers. Nature. 2008;451:949-952.

6. Mayr M. Metabolomics: ready for the prime time? Circ Cardiovasc Genet. 2008;1:58-65.

7. Manicke NE, Nefliu M, Wu C, Woods JW, Reiser V, Hendrickson RC, Cooks RG. Imaging of lipids in atheroma by desorption electrospray ionization mass spectrometry. Anal Chem. 2009;81:8702-8707.

8. Folch J, Lees M, Sloane Stanley GH. A simple method for the isolation and purification of total lipides from animal tissues. J Biol Chem. 1957;226:497-509.

9. Laaksonen R, Katajamaa M, Paiva H, Sysi-Aho M, Saarinen L, Junni P, Lutjohann D, Smet J, Van CR, Seppanen-Laakso T, Lehtimaki T, Soini J, Oresic M. A systems biology strategy reveals biological pathways and plasma biomarker candidates for potentially toxic statin-induced changes in muscle. PLoS One. 2006;1:e97.

10. Graessler J, Schwudke D, Schwarz PE, Herzog R, Shevchenko A, Bornstein SR. Top-down lipidomics reveals ether lipid deficiency in blood plasma of hypertensive patients. PLoS One. 2009;4:e6261.

11. Brugger B, Erben G, Sandhoff R, Wieland FT, Lehmann WD. Quantitative analysis of biological membrane lipids at the low picomole level by nano-electrospray ionization tandem mass spectrometry. Proc Natl Acad Sci U S A. 1997;94:2339-2344.

12. Han X, Gross RW. Global analyses of cellular lipidomes directly from crude extracts of biological samples by ESI mass spectrometry: a bridge to lipidomics. J Lipid Res. 2003;44:1071-1079.

13. Han X, Gross RW. Shotgun lipidomics: electrospray ionization mass spectrometric analysis and quantitation of cellular lipidomes directly from crude extracts of biological samples. Mass Spectrom Rev. 2005;24:367-412.

14. Haimi P, Uphoff A, Hermansson M, Somerharju P. Software tools for analysis of mass spectrometric lipidome data. Anal Chem. 2006;78:8324-8331.

15. Kertesz V, Van Berkel GJ. Fully automated liquid extraction-based surface sampling and ionization using a chip-based robotic nanoelectrospray platform. J Mass Spectrom. 2010;45:252-260.

16. Marshall P, Toteu-Djomte V, Bareille P, Perry H, Brown G, Baumert M, Biggadike K. Correlation of skin blanching and percutaneous absorption for glucocorticoid receptor agonists by matrix-assisted laser desorption ionization mass spectrometry imaging and liquid extraction surface analysis with nanoelectrospray ionization mass spectrometry. Anal Chem. 2010;82:7787-7794.

17. Bottcher C.J.F., Van Gent C.M. Changes in the composition of phospholipids and of phospholipid fatty acids associated with athersoclerosis in the human aortic wall. J Atheroscl Res. 1961;1:36-46.

18. Smith E.B., Cantab B.A. Intimal and medial lipids in human aortas. The Lancet. 1960;276:799-803.

19. Castro-Perez JM, Kamphorst J, Degroot J, Lafeber F, Goshawk J, Yu K, Shockcor JP, Vreeken RJ, Hankemeier T. Comprehensive LC-MS(E) Lipidomic Analysis using a Shotgun Approach and Its Application to Biomarker Detection and Identification in Osteoarthritis Patients. J Proteome Res. 2010;9:2377-2389.

20. Rapp JH, Connor WE, Lin DS, Inahara T, Porter JM. Lipids of human atherosclerotic plaques and xanthomas: clues to the mechanism of plaque progression. J Lipid Res. 1983;24:1329-1335.

21. Blondel VD, Guillaume JL, Lambiotte R, Lefebvre E. Fast unfolding of communities in large networks. Journal of Statistical Mechanics-Theory and Experiment. 2008.

22. Shio H, Haley NJ, Fowler S. Characterization of lipid-laden aortic cells from cholesterol-fed rabbits. III. Intracellular localization of cholesterol and cholesteryl ester. Lab Invest. 1979;41:160-167.

23. Mallat Z, Nakamura T, Ohan J, Leseche G, Tedgui A, Maclouf J, Murphy RC. The relationship of hydroxyeicosatetraenoic acids and F2-isoprostanes to plaque instability in human carotid atherosclerosis. J Clin Invest. 1999;103:421-427.

24. Brown AJ, Leong SL, Dean RT, Jessup W. 7-Hydroperoxycholesterol and its products in oxidized low density lipoprotein and human atherosclerotic plaque. J Lipid Res. 1997;38:1730-1745.

25. Suarna C, Dean RT, May J, Stocker R. Human atherosclerotic plaque contains both oxidized lipids and relatively large amounts of alpha-tocopherol and ascorbate. Arterioscler Thromb Vasc Biol. 1995;15:1616-1624.

26. Witting P, Pettersson K, Ostlund-Lindqvist AM, Westerlund C, Wagberg M, Stocker R. Dissociation of atherogenesis from aortic accumulation of lipid hydro(pero)xides in Watanabe heritable hyperlipidemic rabbits. J Clin Invest. 1999;104:213-220.

27. Degirolamo C, Shelness GS, Rudel LL. LDL cholesteryl oleate as a predictor for atherosclerosis: evidence from human and animal studies on dietary fat. J Lipid Res. 2009;50 Suppl:S434-S439.

28. Serhan CN, Chiang N, Van Dyke TE. Resolving inflammation: dual anti-inflammatory and pro-resolution lipid mediators. Nat Rev Immunol. 2008;8:349-361.

29. Stary HC, Chandler AB, Dinsmore RE, Fuster V, Glagov S, Insull W, Jr., Rosenfeld ME, Schwartz CJ, Wagner WD, Wissler RW. A definition of advanced types of atherosclerotic lesions and a histological classification of atherosclerosis. A report from the Committee on Vascular Lesions of the Council on Arteriosclerosis, American Heart Association. Circulation. 1995;92:1355-1374.

30. Papaspyridonos M, Smith A, Burnand KG, Taylor P, Padayachee S, Suckling KE, James CH, Greaves DR, Patel L. Novel candidate genes in unstable areas of human atherosclerotic plaques. Arterioscler Thromb Vasc Biol. 2006;26:1837-1844.

31. Papaspyridonos M, McNeill E, de Bono JP, Smith A, Burnand KG, Channon KM, Greaves DR. Galectin-3 is an amplifier of inflammation in atherosclerotic plaque progression through macrophage activation and monocyte chemoattraction. Arterioscler Thromb Vasc Biol. 2008;28:433-440.

32. Jiang XC, Paultre F, Pearson TA, Reed RG, Francis CK, Lin M, Berglund L, Tall AR. Plasma sphingomyelin level as a risk factor for coronary artery disease. Arterioscler Thromb Vasc Biol. 2000;20:2614-2618.

33. Auge N, Negre-Salvayre A, Salvayre R, Levade T. Sphingomyelin metabolites in vascular cell signaling and atherogenesis. Prog Lipid Res. 2000;39:207-229.

34. Yeboah J, McNamara C, Jiang XC, Tabas I, Herrington DM, Burke GL, Shea S. Association of plasma sphingomyelin levels and incident coronary heart disease events in an adult population: Multi-Ethnic Study of Atherosclerosis. Arterioscler Thromb Vasc Biol. 2010;30:628-633.

35. Thukkani AK, McHowat J, Hsu FF, Brennan ML, Hazen SL, Ford DA. Identification of alpha-chloro fatty aldehydes and unsaturated lysophosphatidylcholine molecular species in human atherosclerotic lesions. Circulation. 2003;108:3128-3133.

36. Matsumoto T, Kobayashi T, Kamata K. Role of lysophosphatidylcholine (LPC) in atherosclerosis. Curr Med Chem. 2007;14:3209-3220.

37. Barabasi AL, Oltvai ZN. Network biology: understanding the cell's functional organization. Nat Rev Genet. 2004;5:101-113.

38. Dreze M, Charloteaux B, Milstein S, Vidalain PO, Yildirim MA, Zhong Q, Svrzikapa N, Romero V, Laloux G, Brasseur R, Vandenhaute J, Boxem M, Cusick ME, Hill DE, Vidal M. 'Edgetic' perturbation of a C. elegans BCL2 ortholog. Nat Methods. 2009;6:843-849.

39. Carpenter KL, Wilkins GM, Fussell B, Ballantine JA, Taylor SE, Mitchinson MJ, Leake DS. Production of oxidized lipids during modification of low-density lipoprotein by macrophages or copper. Biochem J. 1994;304 (Pt 2):625-633.

40. Carpenter KL, Taylor SE, van d, V, Williamson BK, Ballantine JA, Mitchinson MJ. Lipids and oxidised lipids in human atherosclerotic lesions at different stages of development. Biochim Biophys Acta. 1995;1256:141-150.

41. Upston JM, Niu X, Brown AJ, Mashima R, Wang H, Senthilmohan R, Kettle AJ, Dean RT, Stocker R. Disease stage-dependent accumulation of lipid and protein oxidation products in human atherosclerosis. Am J Pathol. 2002;160:701-710.

42. Carpenter KL, Taylor SE, Ballantine JA, Fussell B, Halliwell B, Mitchinson MJ. Lipids and oxidised lipids in human atheroma and normal aorta. Biochim Biophys Acta. 1993;1167:121-130.

43. Davis B, Koster G, Douet LJ, Scigelova M, Woffendin G, Ward JM, Smith A, Humphries J, Burnand KG, Macphee CH, Postle AD. Electrospray ionization mass spectrometry identifies substrates and products of lipoprotein-associated phospholipase A2 in oxidized human low density lipoprotein. J Biol Chem. 2008;283:6428-6437.

44. Ravandi A, Babaei S, Leung R, Monge JC, Hoppe G, Hoff H, Kamido H, Kuksis A. Phospholipids and oxophospholipids in atherosclerotic plaques at different stages of plaque development. Lipids. 2004;39:97-109.

45. Levkau B. Sphingosine-1-phosphate in the regulation of vascular tone: a finely tuned integration system of S1P sources, receptors, and vascular responsiveness. Circ Res. 2008;103:231-233.

Table 1: Plaque-enriched lipids.

	Lipid species	m/z (positive ion mode)		Lipid species	m/z (positive ion mode)
lPS	lPS(20:0)	554.3	**CE**	CE(10:0)	558.5
PS	PS(38:5)	810.5		CE(14:0)	614.6
	PS(38:2)	816.5		CE(16:1)	640.6
lPC	lPC(14:0)	468.3		CE(18:3)	664.6
	lPC(O-16:0)	482.3		CE(18:1)	668.7
	lPC(O-18:0)	510.3		CE(22:6)	714.5
	lPC(18:2)	520.3		CE(22:5)	716.7
	lPC(22:5)	570.4		CE(22:4)	718.6
	lPC(22:4)	572.3		CE(22:3)	720.7
PC	PC(O-16:0/22:5)	794.5	**PE**	PE(38:3)	770.8
	PC(18:0/20:3)	812.7			

	Lipid species	m/z (negative ion mode)	Lipid species	m/z (negative ion mode)
SM	SM(d18:1/14:0)	709.7 + 733.4	SM(d18:0/15:0)	749.5
	SM(d18:1/15:0)	723.8 + 747.5		

Table 2: Total amount of CE, lPC, PC and SM species in plaques and control arteries.

Lipid class	Endarterectomies (n = 3)	Controls (n = 3)	Δ*
CE	23.95 ± 3.50	0.20 ± 0.10	119.5
lPC	0.36 ± 0.15	0.02 ± 0.01	18.0
PC	3.82 ± 1.05	0.73 ± 0.17	5.2
SM	4.05 ± 1.36	0.27 ± 0.03	15.0

Data presented are given in mg/g tissue (mean±SEM). The total amount was calculated from the fmol/µL and pmol/µL values provided in Supplemental table V using the average molecular weight from all detected species of each lipid class. * Fold enrichment in plaques (n=3) compared to controls (n=3).

Table 3: Quantitation of plaque and plasma cholesteryl esters (CE).

CE species	Asymp-tomatic (n = 6)	Sympto-matic (n = 6)	P value*	Unstable (n = 8)	Stable (n = 8)	P value†	Plasma (n = 35)	P value§
CE(10:0)	0.0 (±0.013)	0.1 (±0.033)	0.480	0.2 (±0.083)	0.1 (±0.025)	0.283	0.0 (±0.000)	**<0.001**
CE(14:0)	0.4 (±0.036)	0.4 (±0.047)	0.689	0.5 (±0.173)	0.3 (±0.031)	0.425	0.3 (±0.016)	**0.015**
CE(16:0)	7.1 (±0.598)	7.1 (±0.204)	0.967	6.3 (±0.284)	6.2 (±0.190)	0.857	6.9 (±0.167)	0.209
CE(16:1)	2.8 (±0.498)	2.5 (±0.211)	0.698	2.8 (±0.393)	2.4 (±0.187)	0.189	2.6 (±0.199)	0.769
CE(18:0)	1.0 (±0.644)	1.1 (±0.738)	0.954	2.1 (±0.799)	0.0 (±0.000)	**0.036**	0.0 (±0.000)	**0.001**
CE(18:1)	25.4 (±1.831)	26.0 (±1.740)	0.826	26.3 (±1.885)	29.2 (±1.247)	0.154	30.0 (±0.446)	**0.001**
CE(18:2)	31.8 (±3.166)	28.1 (±1.755)	0.326	31.2 (±1.655)	27.8 (±1.745)	0.147	41.4 (±0.766)	**<0.001**
CE(18:3)	1.3 (±0.208)	1.2 (±0.222)	0.894	1.7 (±0.242)	1.4 (±0.095)	0.145	1.9 (±0.174)	**0.026**
CE(20:0)	6.4 (±1.323)	6.7 (±1.297)	0.854	3.7 (±0.589)	2.2 (±0.458)	0.058	0.5 (±0.054)	**<0.001**
CE(20:1)	3.3 (±0.131)	4.4 (±0.908)	0.260	2.2 (±0.117)	2.1 (±0.508)	0.789	0.0 (±0.000)	**<0.001**
CE(20:2)	1.1 (±0.155)	2.3 (±0.732)	0.146	1.9 (±0.447)	1.9 (±0.311)	0.991	0.0 (±0.000)	**<0.001**
CE(20:3)	3.1 (±0.380)	4.6 (±0.690)	0.082	3.6 (±0.345)	6.7 (±0.777)	**0.006**	0.0 (±0.000)	**<0.001**
CE(20:4)	9.0 (±0.978)	6.7 (±0.947)	0.114	8.5 (±0.960)	9.4 (±0.850)	0.325	12.6 (±0.738)	**<0.001**
CE(20:5)	3.7 (±0.758)	3.8 (±0.757)	0.935	3.5 (±0.343)	3.3 (±0.302)	0.617	2.5 (±0.235)	**0.002**
CE(22:3)	0.4 (±0.070)	0.6 (±0.078)	0.064	0.8 (±0.359)	0.8 (±0.171)	0.974	0.0 (±0.000)	**<0.001**
CE(22:4)	0.4 (±0.086)	0.8 (±0.152)	**0.037**	0.8 (±0.175)	1.5 (±0.311)	0.053	0.0 (±0.000)	**<0.001**
CE(22:5)	0.8 (±0.168)	1.5 (±0.414)	0.145	1.8 (±0.236)	1.9 (±0.325)	0.525	0.0 (±0.000)	**<0.001**
CE(22:6)	1.9 (±0.267)	2.0 (±0.242)	0.738	2.2 (±0.425)	2.7 (±0.404)	0.262	1.3 (±0.081)	**<0.001**

Data presented are given in % (mean ± SE).

* P values from unpaired t-test for differences between asymptomatic and symptomatic patients.

† P values from paired t-test for differences between stable and ruptured (unstable) areas of the same plaque.

‡ Fold increase/decrease in plaques (n=28) compared with plasma (n=35).

§ P values from unpaired t-test for differences of all plaque (n=28) and plasma samples (n=35).

Figure Legends:

Figure 1. Workflow. **(A)** Using a QqQ-MS, lipids in human endarterectomies were analysed directly from tissue section (LESA) or in Folch extracts. **(B)** Example for a combination of precursor ion scan (m/z = PI 369.3) and FA scans for ammonium adducts of fatty acids to determine CE species. For CE (18:0) at m/z 670.6 and CE (18:1) at m/z 668.6, the identification was hindered by a partial overlap of their peaks. Nonetheless, the presence of CE(18:0) could be clearly demonstrated by the neutral loss of the fatty acid.

Figure 2. LESA compared to lipid extracts. The full MS in positive ion mode **(A)** and head group specific scans for PC (**C**, PI 184.1) and CE species (**E,** PI 369.3) from tissue sections of human endarterectomies. Note the similarity in peak numbers and correlation of signal intensities compared to tissue extracts (**B, D, F**): R^2 = 0.84 for the full MS spectra (**A, B**), R^2 = 0.98 for PCs (**C, D**) and R^2 = 0.99 for CEs (**E,F**).

Figure 3. Endarterectomies versus radial arteries. **(A)** Full MS scans in positive ion mode for 3 control radial arteries (C1-3) and 3 endarterectomies (P1-3). **(B)** Comparison between patient samples P1, P2 and P3 (left panel) and control samples C1, C2 and C3 (right panel) for their CE head group scan at m/z 369.3.

Figure 4. Plaque-enriched CE species. **(A)** Quantification of CE species in plaque and control samples with CE(19:0) as internal standard. **(B)** Relative distribution of CE in atherosclerotic plaques compared with control arteries. Plaque-specific CE species are highlighted in colour.

Figure 5: Plaque heterogeneity. PCAs for lipid profiles of ruptured and non-ruptured areas of the same symptomatic plaques (see inset for macroscopic classification). The green circles denote non-ruptured areas (S, stable) and the red squares ruptured areas (U, unstable) of the same lesion. The numbers correspond to the patients (P) in **Supplemental Table VII**.

Figure 6: Differential lipid profile in plaque and plasma samples. **A)** Principal component analysis (PCA) of 87 lipid species across plaque (n = 28) and plasma (n = 35). Magnitude and sign of the contribution of each lipid to the first three principal components is visualized as blue lines. **B)** Lipid importance for differentiating plaque and plasma samples. Higher values are indicative of greater importance.

Figure 7: Systems-wide relationships between lipids involved in atherosclerosis. Lipid-lipid co-expression network where each node represents a lipid and each edge a correlation in expression between two lipid pairs. Only lipid pairs with Pearson correlation coefficient ≥ 0.70 were included in the network. Lipids and co-expressions specific for the asymptomatic-symptomatic phenotype (**A**) are represented as triangles and red links, respectively, while lipids and co-expressions specific for the stable-unstable network (**B**) are represented as diamonds and blue links. Lipids and co-expressions common to both phenotypes are represented as circles and black edges. Lipid colors correspond to unique clusters, computed using an unbiased network clustering algorithm.[21]

A

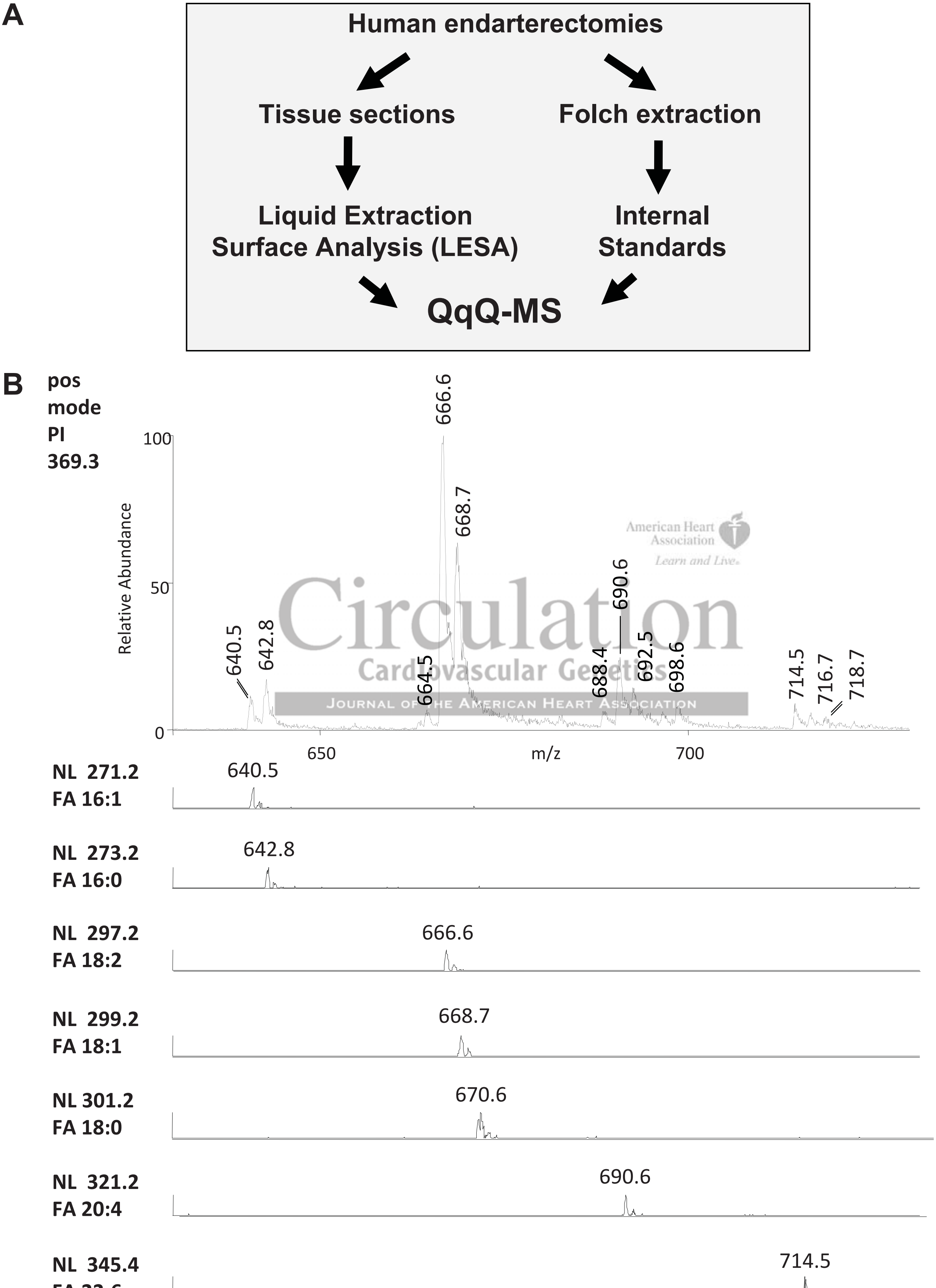
Human endarterectomies
Tissue sections
Folch extraction
Liquid Extraction
Surface Analysis (LESA)
Internal
Standards
QqQ-MS
B
pos
mode
PI
369.3
Relative Abundance
100
50
0
666.6
668.7
640.5
642.8
664.5
688.4
690.6
692.5
698.6
714.5
716.7
718.7
650
m/z
700
NL 271.2
FA 16:1
640.5
NL 273.2
FA 16:0
642.8
NL 297.2
FA 18:2
666.6
NL 299.2
FA 18:1
668.7
NL 301.2
FA 18:0
670.6
NL 321.2
FA 20:4
690.6
NL 345.4
FA 22:6
714.5

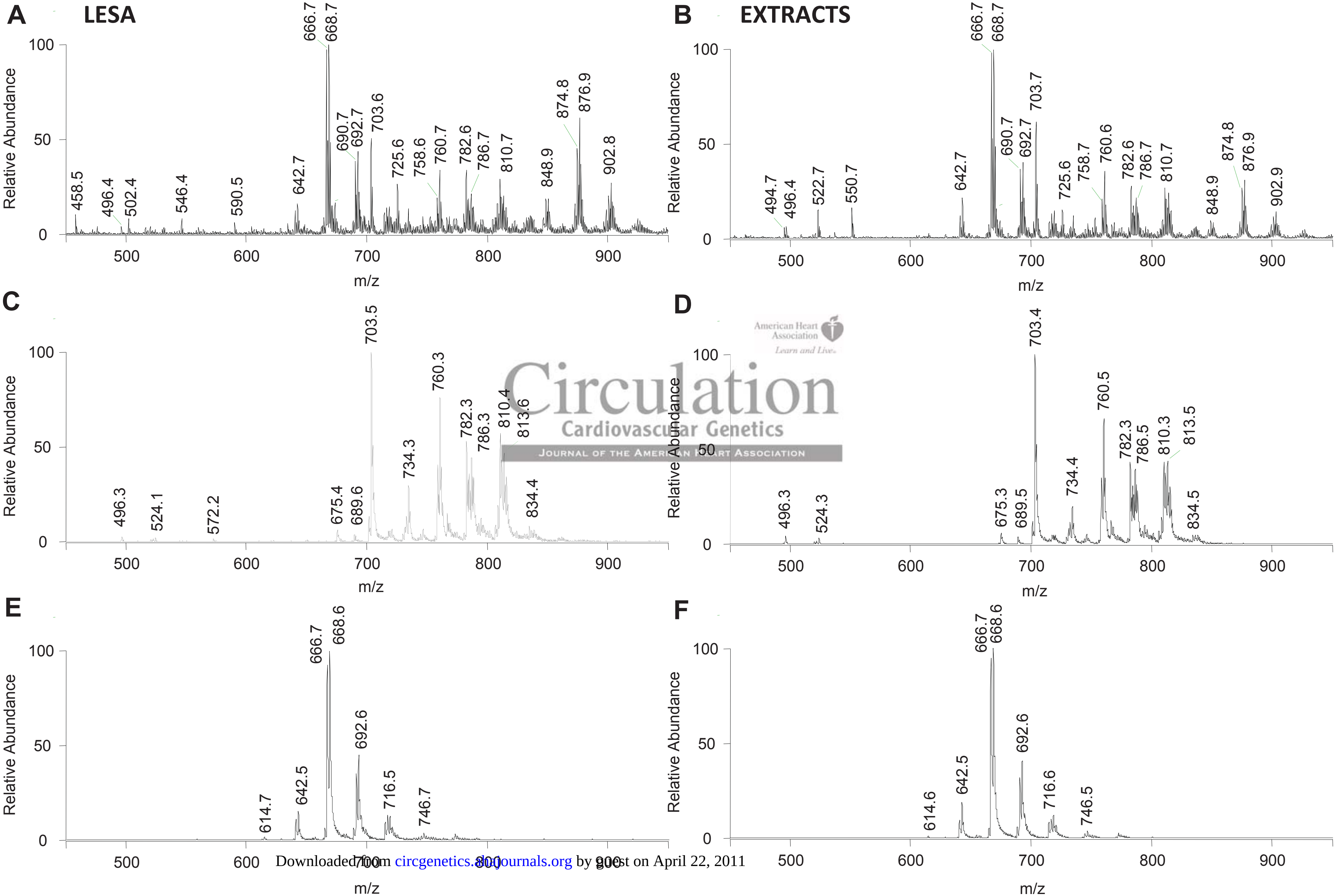
A
LESA
B
EXTRACTS
C
D
E
F
Relative Abundance
m/z
458.5
496.4
502.4
546.4
590.5
642.7
666.7
668.7
690.7
692.7
703.6
725.6
758.6
760.7
782.6
786.7
810.7
848.9
874.8
876.9
902.8
494.7
496.4
522.7
550.7
642.7
666.7
668.7
690.7
692.7
703.7
725.6
758.7
760.6
782.6
786.7
810.7
848.9
874.8
876.9
902.9
496.3
524.1
572.2
675.4
689.6
703.5
734.3
760.3
782.3
786.3
810.4
813.6
834.4
496.3
524.3
675.3
689.5
703.4
734.4
760.5
782.3
786.5
810.3
813.5
834.5
614.7
642.5
666.7
668.6
692.6
716.5
746.7
614.6
642.5
666.7
668.6
692.6
716.6
746.5

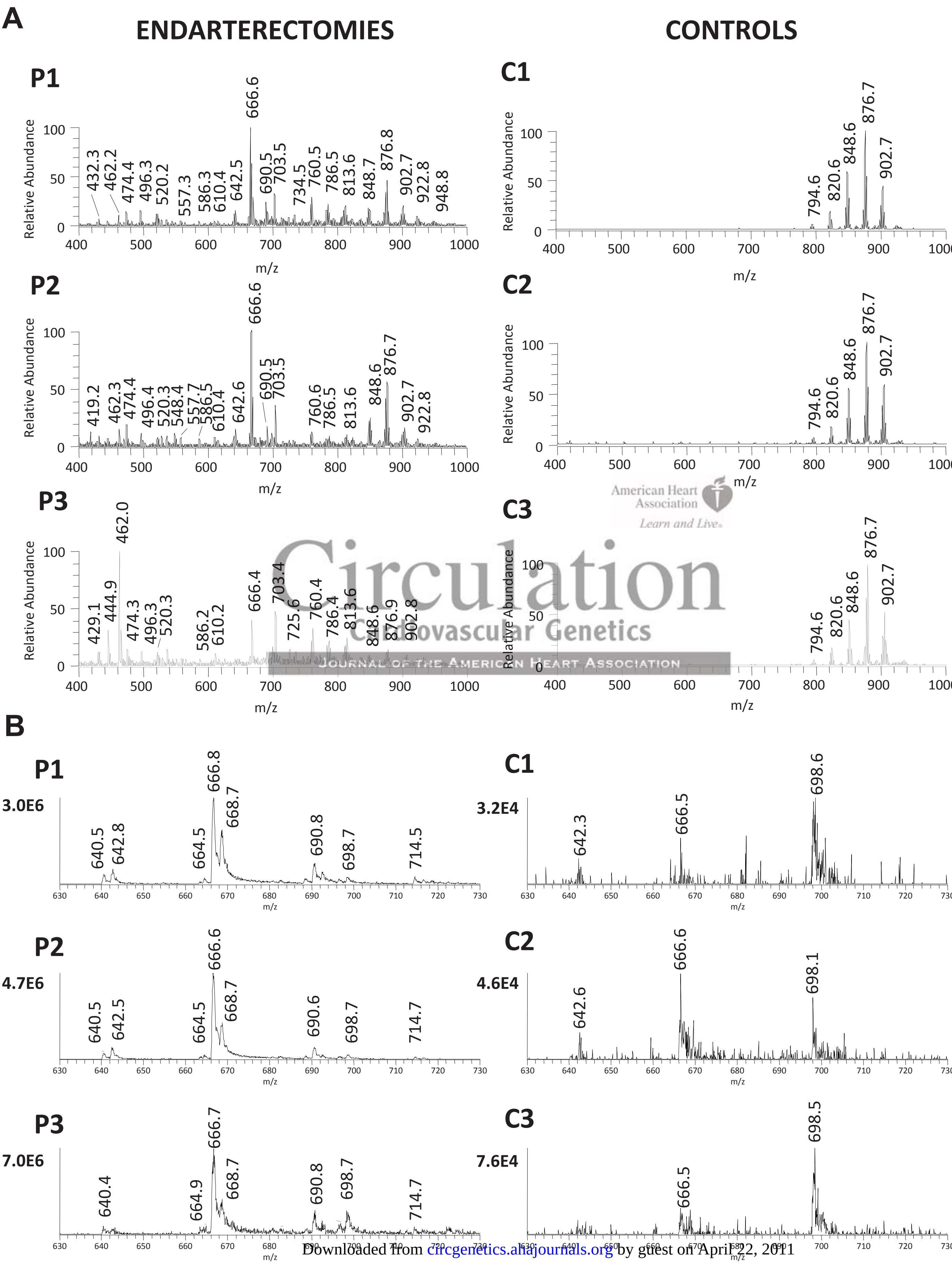
A
ENDARTERECTOMIES
CONTROLS
P1
666.6
432.3
462.2
474.4
496.3
520.2
557.3
586.3
610.4
642.5
690.5
703.5
734.5
760.5
786.5
813.6
848.7
876.8
902.7
922.8
948.8
Relative Abundance
m/z
C1
794.6
820.6
848.6
876.7
902.7
P2
666.6
419.2
462.3
474.4
496.4
520.3
548.4
557.7
586.5
610.4
642.6
690.5
703.5
760.6
786.5
813.6
848.6
876.7
902.7
922.8
C2
794.6
820.6
848.6
876.7
902.7
P3
462.0
429.1
444.9
474.3
496.3
520.3
586.2
610.2
666.4
703.4
725.6
760.4
786.4
813.6
848.6
876.9
902.8
C3
794.6
820.6
848.6
876.7
902.7
B
P1
3.0E6
640.5
642.8
664.5
666.8
668.7
690.8
698.7
714.5
C1
3.2E4
642.3
666.5
698.6
P2
4.7E6
640.5
642.5
664.5
666.6
668.7
690.6
698.7
714.7
C2
4.6E4
642.6
666.6
698.1
P3
7.0E6
640.4
664.9
666.7
668.7
690.8
698.7
714.7
C3
7.6E4
666.5
698.5

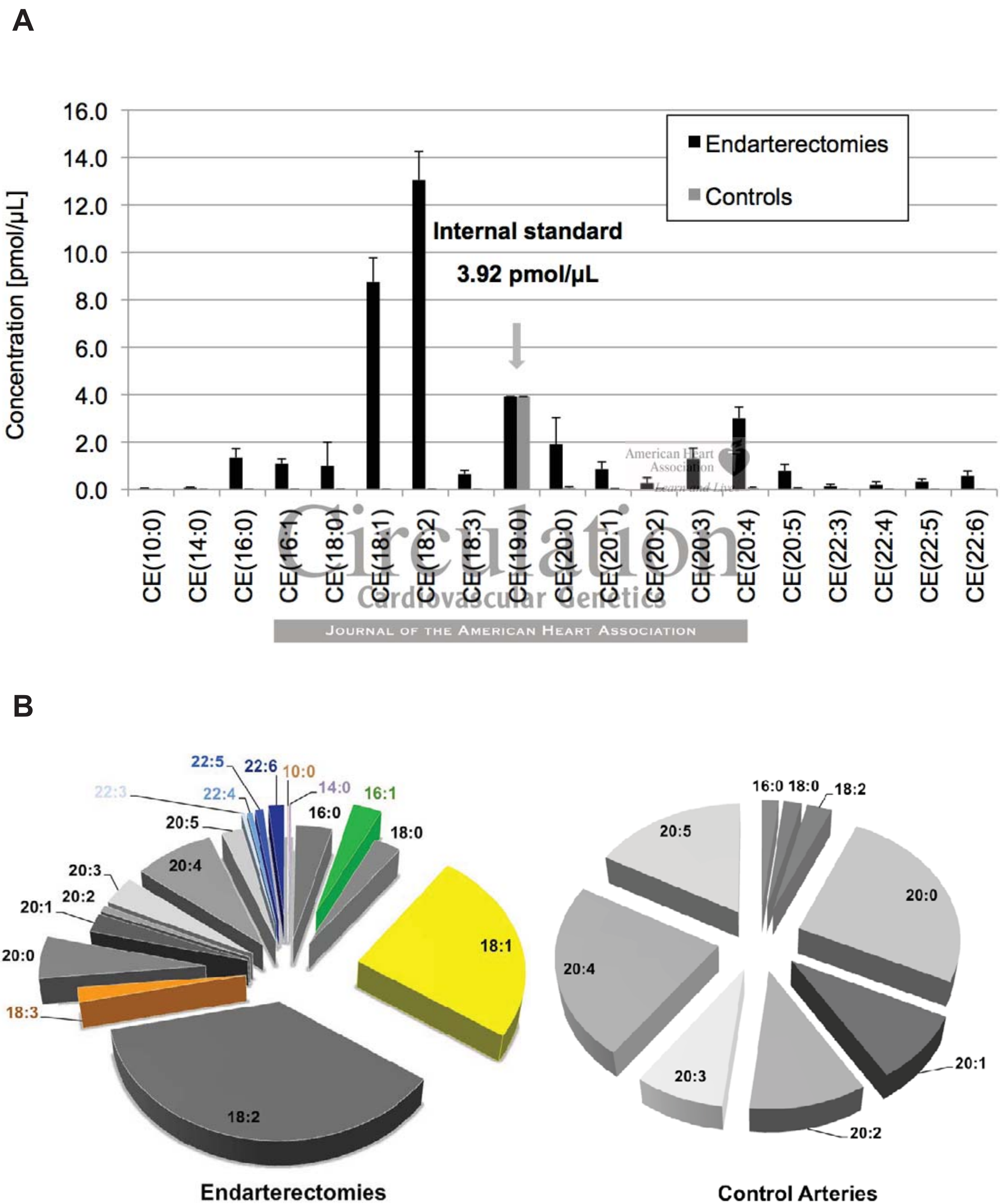
A
16.0
14.0
12.0
10.0
8.0
6.0
4.0
2.0
0.0
Concentration [pmol/µL]
Endarterectomies
Controls
Internal standard
3.92 pmol/µL
CE(10:0)
CE(14:0)
CE(16:0)
CE(16:1)
CE(18:0)
CE(18:1)
CE(18:2)
CE(18:3)
CE(19:0)
CE(20:0)
CE(20:1)
CE(20:2)
CE(20:3)
CE(20:4)
CE(20:5)
CE(22:3)
CE(22:4)
CE(22:5)
CE(22:6)
B
22:5
22:6
10:0
22:3
22:4
14:0
16:1
16:0
20:5
18:0
20:4
20:3
20:2
20:1
18:1
20:0
18:3
18:2
Endarterectomies
16:0
18:0
18:2
20:5
20:0
20:4
20:3
20:1
20:2
Control Arteries

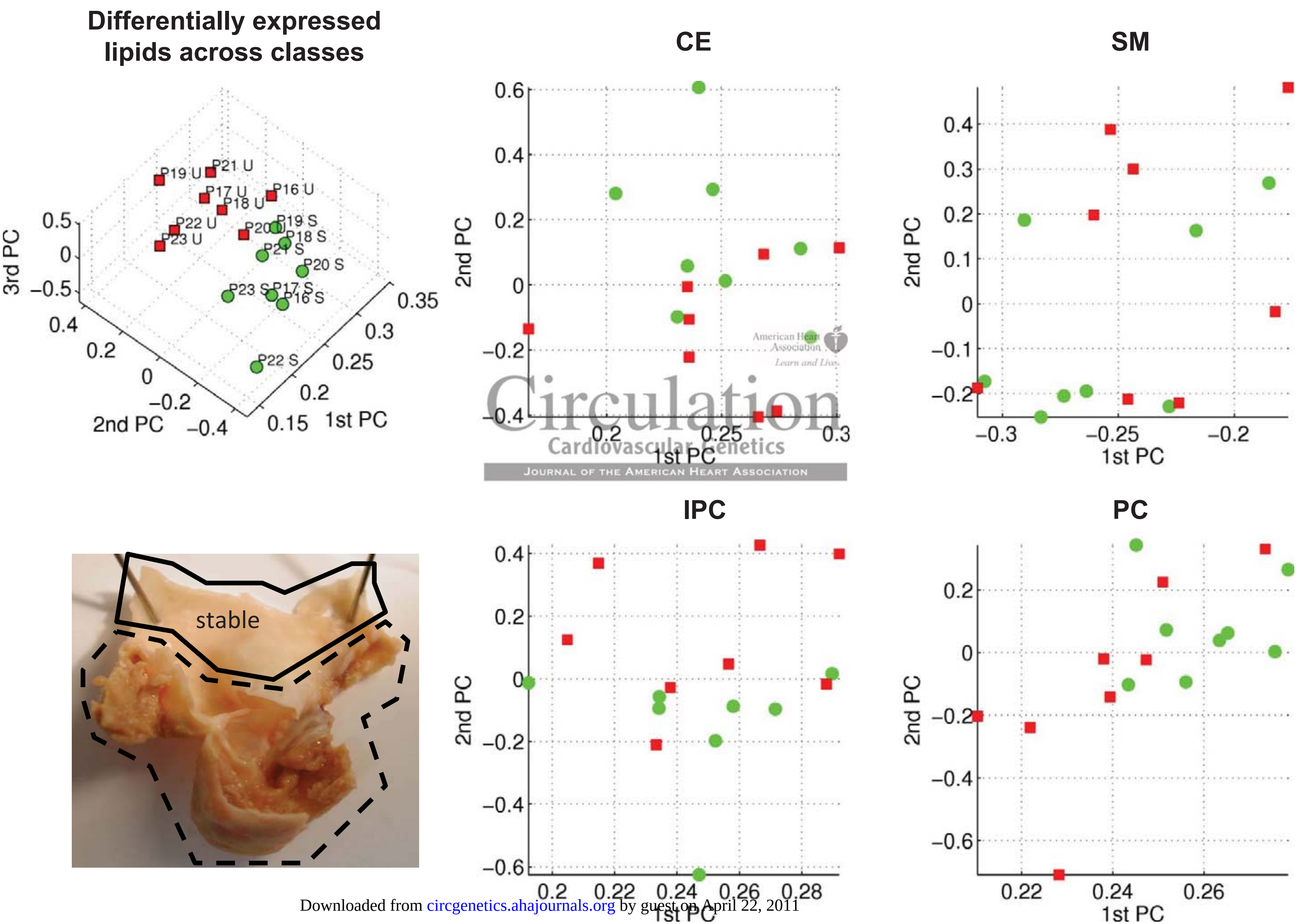
Differentially expressed lipids across classes
P19 U
P21 U
P17 U
P16 U
P18 U
P22 U
P23 U
P20 U
P19 S
P18 S
P21 S
P20 S
P23 S
P17 S
P16 S
P22 S
3rd PC
2nd PC
1st PC
CE
SM
IPC
PC
2nd PC
1st PC
stable

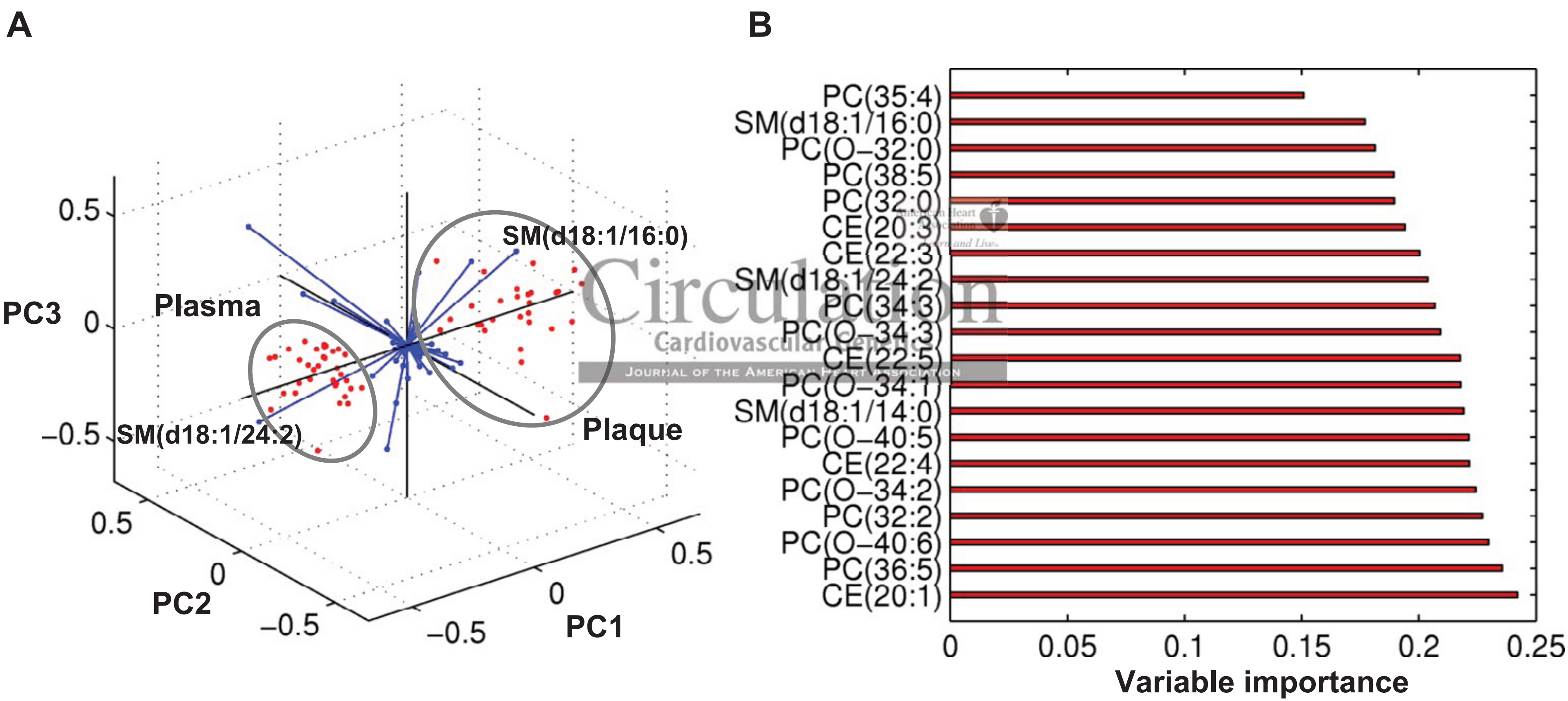
A
PC3
Plasma
Plaque
SM(d18:1/16:0)
SM(d18:1/24:2)
PC1
PC2
0.5
0
−0.5
B
PC(35:4)
SM(d18:1/16:0)
PC(O−32:0)
PC(38:5)
PC(32:0)
CE(20:3)
CE(22:3)
SM(d18:1/24:2)
PC(34:3)
PC(O−34:3)
CE(22:5)
PC(O−34:1)
SM(d18:1/14:0)
PC(O−40:5)
CE(22:4)
PC(O−34:2)
PC(32:2)
PC(O−40:6)
PC(36:5)
CE(20:1)
0
0.05
0.1
0.15
0.2
0.25
Variable importance

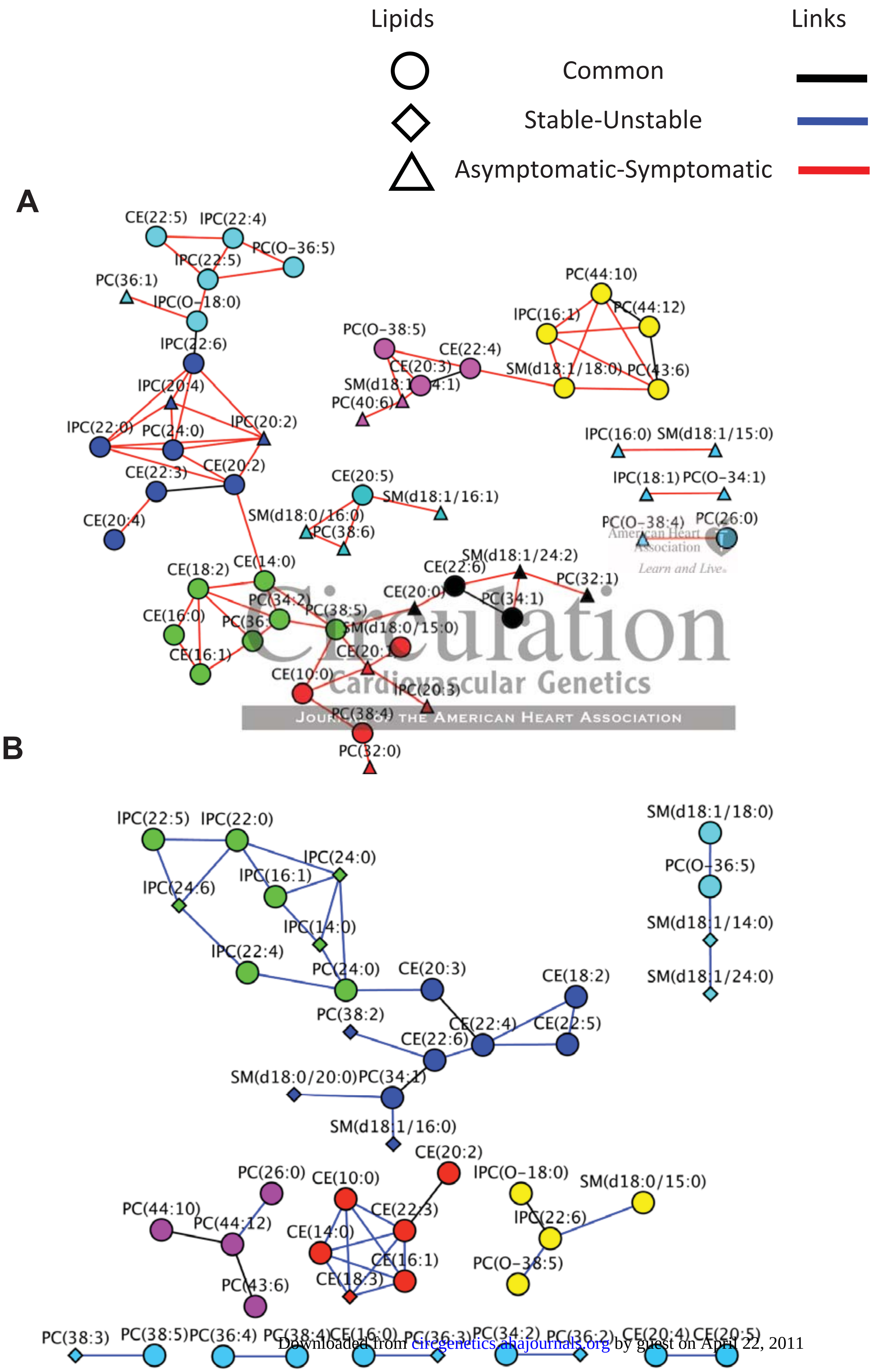

Lipids
Links
Common
Stable-Unstable
Asymptomatic-Symptomatic
A
CE(22:5)
IPC(22:4)
PC(O−36:5)
IPC(22:5)
PC(36:1)
IPC(O−18:0)
IPC(22:6)
IPC(20:4)
IPC(22:0)
PC(24:0)
IPC(20:2)
CE(22:3)
CE(20:2)
CE(20:4)
PC(O−38:5)
CE(22:4)
CE(20:3)
PC(40:6)
PC(44:10)
IPC(16:1)
PC(44:12)
SM(d18:1/18:0)
PC(43:6)
IPC(16:0)
SM(d18:1/15:0)
IPC(18:1)
PC(O−34:1)
CE(20:5)
SM(d18:1/16:1)
SM(d18:0/16:0)
PC(38:6)
PC(O−38:4)
PC(26:0)
SM(d18:1/24:2)
CE(22:6)
PC(32:1)
CE(20:0)
PC(34:1)
CE(18:2)
CE(14:0)
PC(34:2)
CE(16:0)
PC(38:5)
SM(d18:0/15:0)
CE(16:1)
CE(10:0)
IPC(20:3)
PC(38:4)
PC(32:0)
B
IPC(22:5)
IPC(22:0)
IPC(24:0)
IPC(16:1)
IPC(24:6)
IPC(14:0)
IPC(22:4)
PC(24:0)
CE(20:3)
CE(18:2)
PC(38:2)
CE(22:4)
CE(22:5)
CE(22:6)
SM(d18:0/20:0)
PC(34:1)
SM(d18:1/16:0)
SM(d18:1/18:0)
PC(O−36:5)
SM(d18:1/14:0)
SM(d18:1/24:0)
CE(20:2)
PC(26:0)
CE(10:0)
IPC(O−18:0)
SM(d18:0/15:0)
PC(44:10)
PC(44:12)
CE(22:3)
IPC(22:6)
CE(14:0)
CE(16:1)
PC(O−38:5)
CE(18:3)
PC(43:6)
PC(38:3)
PC(38:5)
PC(36:4)
PC(38:4)
CE(16:0)
PC(36:3)
PC(34:2)
PC(36:2)
CE(20:4)
CE(20:5)

SUPPLEMENTAL MATERIAL

Supplemental Methods

Lipid extraction. Tissue was pulverized with a mortar and pestle or a ball-grinding method (Mikro Dismembrator, Sartorius). All subsequent steps were performed in glass vials that were thoroughly rinsed with water, methanol, and chloroform before use. 300 μL water (HPLC grade, Fisher Scientific), 2 mL methanol (HPLC grade, Fisher Scientific) and 4 mL chloroform (GLC-pesticide residue grade, Fisher Scientific) were added to each sample. Then, the mixture was vortexed for 10 min and centrifuged for 10 min at 3000 rpm. The supernatant was transferred, mixed with 1.2 mL water and vortexed for 10 min. After centrifugation at 1000 rpm for 5 min the lower organic phase was transferred into a new glass vial and 2 ml of chloroform/methanol/water (3:48:47) was added. To extract any remaining lipids, the upper phase was washed with 2 mL chloroform and centrifuged for 5 min at 1000 rpm. The two organic phases were combined and split into aliquots corresponding to 50 mg of tissue. The organic solvent was evaporated and samples stored at -80°C.

Plasma extraction. 10 μL of plasma were added to an aliquot (110 μL) of an internal standard mixture in a glass vial. 10 μL 0.15 M sodium chloride were added and each sample was homogenized by vortexing for 5 sec. After 30 min incubation at room temperature the samples were centrifuged for 3 min at 10000 rpm and an exact aliquot of the lower phase (50 μL) was transferred in a new glass vial. The internal standard mixture included 2600 pmol CE(17:0), 750 pmol lPC(19:0), 5000 pmol PC(17:0/17:0) and 750 pmol SM(d18:1/12:0) (all Avanti polar lipids, Alabaster, AL) in chlorform/methanol 2:1 containing butylated hydroxytoluene (BHT, 20 mg/L).

Network analysis. The PCC threshold was set to >0.70 on the basis of the following evidence: (i) -omic correlation profiles with PCC over 0.60 were demonstrated to be more biologically relevant[1] and (ii) below this cut-off all networks were excessively large (>700 co-expressions), suggesting a presence of false-positive edges. A more stringent PCC threshold was avoided due to rapid elimination of most lipid co-expressions. For the unbiased network clustering algorithm we used the Louvain Method for fast community detection in graphs. The algorithm is parameter-free and identifies community structures by maximizing network modularity.[2]

Supplemental References

1. Elo LL, Jarenpaa H, Oresic M, Lahesmaa R, Aittokallio T. Systematic construction of gene coexpression networks with apllications to human T helper cell differentiation process. Bioinformatics 2007;23, 2096-2103.
2. Newman MEJ. Modularity and community structure in networks. Proc Natl Acad Sci. 2006;103, 8577-8582.
3. Manicke NE, Nefliu M, Wu C, Woods JW, Reiser V, Hendrickson RC, Cooks RG. Imaging of lipids in atheroma by desorption electrospray ionization mass spectrometry. Anal Chem. 2009;81:8702-8707.

Supplemental Figures

Supplemental Figure I: A full MS scan **(A)** and a PI scan at m/z 168.0 for SM species **(B)** in negative ion mode.

Supplemental Figure II: PCAs for lipid profiles of symptomatic and asymptomatic patients. The red circles denote symptomatic patients; the blue squares denote asymptomatic patients. The numbers correspond to the patients in **Supplemental Table VI**. The plot on the right show the magnitude of the first 2 principal components based on all measurements. The black and green lines represent the mean value of the weights in symptomatic and asymptomatic plaques. CE and, to lesser, extent SM, contributed to most of the composition of the first two principal components.

Supplemental Figure III: Comparison of relative distribution of CE species in plasma (n = 35) and plaques (n = 28).

Supplemental Figure IV: Comparison of relative distribution of SM species in plasma (n = 35) and plaques (n = 28).

Supplemental Figure V: Comparison of relative distribution of IPC species in plasma (n = 35) and plaques (n = 28).

Supplemental Figure VI: Comparison of relative distribution of PC species in plasma (n = 35) and plaques (n = 28).

Supplemental Table I: Neutral loss (NL) and precursor ion (PI) scans plus their collision energy (CE) used for shotgun lipidomics on a QqQ-MS (TSQ Vantage, ThermoFisher).

Lipid class	Precursor ion	MS mode	MS/MS mode	CE (eV)
PC, lysoPC, SM	$[M+H]^+$	pos	PI 184.1	30
acylcarnitine	$[M+H]^+$	pos	PI 85.1	20
CE	$[M+NH_4]^+$	pos	PI 369.3	20
PE	$[M+H]^+$	pos	NL 141.0	25
PS	$[M+H]^+$	pos	NL 185.0	22
scans for different FAs from TAG+CE species	$[M+NH_4]^+$	pos	NL + NH_4	35
PC, lysoPC, SM	$[M-Cl]^-$	neg	NL 50.0	24
PS	$[M-H]^-$	neg	NL 87.0	28
Glycerophospholipids	$[M-H]^-$	neg	PI 153.0	50
PI	$[M-H]^-$	neg	PI 241.0	45
PIP	$[M-H]^-$	neg	PI 321.1	53
PIP_2	$[M-H]^-$	neg	PI 401.1	62
Sulfatides	$[M-H]^-$	neg	PI 97.0	65
acylCoA	$[M-2H]^{2-}$	neg	PI 339.0	30
Ceramide (non-hydroxy)	$[M-H]^-$	neg	NL 256.0	32
Ceramide (2-hydroxy)	$[M-H]^-$	neg	PI 327.3	32
Ceramide (general)	$[M-H]^-$	neg	NL 240.2	32
Cerebroside	$[M-Cl]^-$	neg	NL 36.0	30
SM	$[M-H]^-$	neg	PI 168.0	35
scans for different FAs from PC species	$[M-Ac]^-$	neg	PI	28

Supplemental Table II: Clinical characteristics from patients undergoing endarterectomy and control subjects.

	Age	Gender	BMI	DM	COPD	HTN	Renal failure	b-blockers	ASA	ACEI	Statins
Patient 1	66	Male	21	No	No	Yes	No	No	Yes	No	Yes
Patient 2	82	Male	23	No	No	Yes	No	No	No	No	No
Patient 3	70	Male	26	No	No	Yes	No	Yes	Yes	Yes	No
Control 1	60	Male	27	No	No	Yes	No	No	Yes	No	Yes
Control 2	61	Male	26	No	No	No	No	Yes	Yes	Yes	Yes
Control 3	55	Male	24	No	No	Yes	No	Yes	Yes	Yes	Yes

Patient 1 and 3 were undergoing carotid endartectomy, Patient 2 was undergoing femoral endarterectomy, and macroscopically normal radial arteries from individuals undergoing coronary bypass grafting were used as controls
BMI indicates body mass index; DM, diabetes mellitus; COPD, Chronic obstructive pulmonary disease; HTN, hypertension; ASA, acetyl salicylic acid; ACEI, angiotensin-converting enzyme inhibitors.

Supplement Table III: **Lipids identified in endarterectomies (P1-P3) and radial control arteries (C1-C3) in positive MS mode.**

	m/z	Lipid	P1	P2	P3	C1	C2	C3
IPE	454.4	IPE(16:0)	✓	✓	---	---	✓	---
	480.4	IPE(18:1)	✓	✓	---	---	✓	✓
	482.2	IPE(18:0)[L]	✓	✓	---	---	✓	---
	526.3	IPE(22:6)	---	---	---	---	✓	---
	528.4	IPE(22:5)[L]	---	---	---	---	✓	✓
	530.4	IPE(22:4)[L]	✓	✓	---	---	✓	---
	554.4	IPE(24:6)[L]	✓	✓	---	---	✓	---
	556.4	IPE(24:5)[L]	✓	✓	---	---	--	✓
	558.5	IPE(24:4)[L]	✓	✓	---	---	---	---
	566.5	IPE(24:0)	✓	✓	---	---	✓	---
PE	636.5	PE(28:0)	✓	---	---	---	---	---
	716.6	PE(34:2)[L]	✓	✓	✓	---	✓	✓
	718.5	PE(34:1)[L]	✓	✓	✓	✓	✓	✓
	724.9	PE(O-36:5)[L]	✓	---	✓	---	✓	---
	740.6	PE(36:4)[L]	✓	✓	✓	---	✓	---
	742.5	PE(36:3)[L]	✓	✓	✓	✓	✓	---
	744.5	PE(36:2)[L]	✓	✓	---	---	✓	✓
	746.6	PE(36:1)[L]	✓	✓	✓	✓	✓	✓
	762.5	PE(O-38:0)	---	---	---	---	✓	---
	764.6	PE(38:6)[L]	✓	✓	✓	---	✓	---
	766.5	PE(38:5)[L]	✓	✓	---	---	✓	---
	768.5	PE(38:4)[L]	✓	✓	✓	✓	✓	--
	770.8	PE(38:3)[L]	✓	✓	✓	---	---	---
	790.7	PE(O-40:0)[L]	✓	---	---	---	✓	---
	792.6	PE(40:6)[L]	✓	✓	✓	---	✓	---
	794.7	PE(40:5)[L]	✓	✓	✓	---	✓	---
	796.7	PE(40:4)[L]	✓	✓	✓	---	✓	---
IPS	526.3	IPS(18:0)	✓	✓	---	---	---	---
	554.3	IPS(20:0)[L]	✓	✓	✓	---	---	---
PS	762.8	PS(34:1)	✓	---	---	✓	✓	✓
	764.6	PS(34:0)	✓	---	---	---	✓	---
	788.6	PS(36:2)[L]	✓	✓	---	✓	✓	---
	790.5	PS(36:1)[L]	✓	✓	✓	✓	---	✓
	792.6	PS(36:0)[L]	✓	---	---	✓	✓	✓

	810.8	PS(38:5)[L]	✓	✓	✓	---	---	---
	812.8	PS(38:4)[L]	✓	✓	✓	✓	✓	---
	814.6	PS(38:3)[L]	✓	✓	✓	✓	✓	---
	816.5	PS(38:2)[L]	✓	✓	✓	---	---	---
	836.7	PS(40:6)[L]	✓	✓	✓	✓	✓	---
	838.6	PS(40:5)[L]	✓	✓	---	---	✓	---
	840.5	PS(40:4)[L]	✓	✓	---	---	✓	---
SM	675.5	SM(d18:1/14:0)[L] *	✓	✓	✓	✓	✓	---
	689.4	SM(d18:1/15:0)[L] *	✓	✓	✓	---	---	---
	701.6	SM(d18:1/16:1)[L] *	✓	✓	✓	✓	✓	✓
	703.7	SM(d18:1/16:0)[L] *	✓	✓	✓	✓	✓	✓
	705.5	SM(d18:0/16:0)[L]	✓	✓	✓	---	---	---
	731.6	SM(d18:1/18:0)[L] *	✓	✓	✓	---	✓	✓
	811.7	SM(d18:1/24:2)[L] *	✓	✓	✓	✓	---	✓
	813.8	SM(d18:1/24:1)[L] *	✓	✓	✓	✓	✓	✓
	815.7	SM(d18:1/24:0)[L]	✓	✓	✓	✓	✓	✓
IPC	468.3	IPC(14:0)[L]	✓	✓	✓	---	---	---
	480.2	IPC(O-16:1)[L]	✓	---	---	---	---	---
	482.3	IPC(O-16:0)[L]	✓	✓	✓	---	---	---
	494.4	IPC(16:1)[L]	✓	---	---	---	---	---
	496.3	IPC(16:0)[L] *	✓	✓	✓	✓	✓	✓
	510.3	IPC(O-18:0)	✓	✓	✓	---	---	---
	520.3	IPC(18:2)[L] *	✓	✓	✓	---	---	---
	522.4	IPC(18:1)[L] *	✓	✓	✓	---	✓	✓
	524.5	IPC(18:0)[L] *	✓	✓	✓	---	✓	✓
	544.4	IPC(20:4)[L]	✓	---	✓	---	✓	---
	546.3	IPC(20:3)[L]	✓	---	---	---	---	---
	548.3	IPC(20:2)[L]	✓	---	---	---	---	---
	568.4	IPC(22:6)	✓	✓		---	✓	---
	570.4	IPC(22:5)[L]	✓	✓	✓	---	---	---
	572.3	IPC(22:4)[L]	✓	✓	✓	---	---	---
	580.4	IPC(22:0)[L]	✓	✓	---	---	✓	---
	596.3	IPC(24:6)	✓	✓	---	✓	✓	---
	608.5	IPC(24:0)	✓	✓	---	---	✓	---
PC	594.5	PC(22:0)[L]	✓	✓	✓	✓	✓	✓
	622.5	PC(24:0)[L]	✓	✓	✓	✓	✓	✓
	650.5	PC(26:0)[L]	✓	✓	✓	✓	✓	✓
	732.6	PC(16:0/16:1)[L]	✓	✓	✓	✓	✓	✓

	734.5	PC(16:0/16:0)^{L} *	✓	✓	✓	✓	✓	✓
	746.5	PC(O-34:1)^{L} *	✓	✓	✓	---	✓	---
	758.6	PC(18:2/16:0)^{L} *	✓	✓	✓	✓	✓	✓
	760.6	PC(16:0/18:1)^{L} *	✓	✓	✓	✓	✓	✓
	766.7	PC(O-16:1/20:4)^{L}	✓	---	✓	---	✓	---
	768.5	PC(O-16:0/20:4)^{L}	✓	---	✓	---	---	---
	782.5	PC(16:0/20:4)^{L} *	✓	✓	✓	✓	✓	---
	784.6	PC(18:1/18:2)^{L} *	✓	✓	✓	✓	✓	✓
	786.5	PC(18:0/18:2)^{L} * PC(18:1/18:1)^{L} *	✓	✓	✓	✓	✓	✓
	788.7	PC(18:0/18:1)^{L}	✓	✓	✓	✓	✓	✓
	794.5	PC(O-16:0/22:5)^{L}	✓	✓	✓	---	---	---
	796.6	PC(O-38:4)^{L}	✓	---	---	---	---	---
	806.6	PC(16:0/22:6)^{L}	✓	✓	✓	✓	✓	---
	808.6	PC(18:1/20:4)^{L}	✓	✓	✓	✓	✓	---
	810.6	PC(18:0/20:4)^{L}	✓	✓	✓	✓	✓	---
	812.7	PC(18:0/20:3)^{L}	✓	✓	✓	---	---	---
	814.7	PC(38:2)^{L}	✓	✓	✓	---	✓	---
	834.6	PC(40:6)^{L}	✓	✓	---	---	✓	---
	836.7	PC(18:0/22:5)^{L}	✓	✓	---	---	✓	---
	838.7	PC(40:4)^{L}	✓	✓	---	---	---	---
	876.6	PC(43:6)	✓	---	---	---	---	---
	878.6	PC(44:12)^{L}	✓	---	---	---	---	---
CE	558.5	CE(10:0)^{L}	✓	✓	✓	---	---	---
	614.6	CE(14:0)^{L}	✓	✓	✓	---	---	---
	640.6	CE(16:1)^{L} *	✓	✓	✓	---	---	---
	642.6	CE(16:0)^{L} *	✓	✓	✓	✓	---	---
	664.6	CE(18:3)^{L}	✓	✓	✓	---	---	---
	666.7	CE(18:2)^{L} *	✓	✓	✓	✓	✓	---
	668.6	CE(18:1)^{L} *	✓	✓	✓	---	---	---
	670.6	CE(18:0)	✓	✓	✓	✓	---	---
	688.6	CE(20:5)^{L}	✓	✓	✓	---	---	✓
	690.7	CE(20:4)^{L} *	✓	✓	✓	---	---	✓
	692.6	CE(20:3)^{L} *	✓	✓	✓	---	---	✓
	694.6	CE(20:2)^{L}	✓	✓	✓	---	---	✓
	696.7	CE(20:1)	✓	✓	✓	---	---	✓
	698.6	CE(20:0)^{L}	✓	✓	✓	✓	✓	✓
	714.7	CE(22:6)^{L}	✓	✓	✓	---	---	---

	716.7	CE(22:5)[L]	✓	✓	✓	---	---	---
	718.7	CE(22:4)[L]	✓	✓	✓	---	---	---
	720.7	CE(22:3)[L]	✓	✓	✓	---	---	---
TAG	792.6	TAG(46:2)[L]	✓	✓	✓	✓	✓	✓
	794.6	TAG(46:1)[L]	✓	✓	✓	✓	✓	✓
	796.6	TAG(46:0)[L]	✓	✓	✓	✓	✓	✓
	818.6	TAG(48:3)	✓	---	✓	✓	✓	✓
	820.6	TAG(48:2)[L]	✓	✓	✓	✓	✓	✓
	822.6	TAG(48:1)[L]	✓	✓	✓	✓	✓	✓
	824.6	TAG(48:0)[L]	✓	✓	✓	✓	✓	✓
	844.6	TAG(50:4)	✓	✓	---	✓	✓	✓
	846.6	TAG(50:3)[L]	✓	✓	✓	✓	✓	✓
	848.6	TAG(50:2)[L]	✓	✓	✓	✓	✓	✓
	850.7	TAG(50:1)[L]	✓	✓	✓	✓	✓	✓
	862.7	TAG(O-52:2)	✓	✓	✓	✓	✓	✓
	870.6	TAG(52:5)	✓	✓	---	✓	✓	✓
	872.6	TAG(52:4)[L]	✓	✓	✓	✓	✓	✓
	874.7	TAG(52:3)[L]	✓	✓	✓	✓	✓	✓
	876.8	TAG(52:2)[L]	✓	✓	✓	✓	✓	✓
	878.7	TAG(52:1)[L]	✓	✓	✓	✓	✓	✓
	896.7	TAG(54:6)[L]	✓	✓	---	✓	✓	✓
	898.7	TAG(54:5)[L]	✓	✓	✓	✓	✓	✓
	900.7	TAG(54:4)[L]	✓	✓	✓	✓	✓	✓
	902.7	TAG(54:3)[L]	✓	✓	✓	✓	✓	✓
	904.8	TAG(54:2)[L]	✓	✓	✓	✓	✓	✓
	906.7	TAG(54:1)[L]	✓	✓	✓	✓	✓	✓
	920.7	TAG(56:8)[L]	✓	✓	✓	✓	---	✓
	922.8	TAG(56:7)[L]	✓	✓	✓	✓	✓	✓
	924.8	TAG(56:6)[L]	✓	✓	---	✓	✓	✓
	926.7	TAG(56:5)[L]	✓	✓	---	✓	✓	✓
	928.7	TAG(56:4)[L]	✓	---	✓	✓	✓	✓
	930.7	TAG(56:3)[L]	✓	---	✓	✓	✓	✓
	946.7	TAG(58:9)	✓	---	---	✓	---	✓
	948.8	TAG(58:8)	✓	---	---	✓	✓	✓
	950.8	TAG(58:7)[L]	✓	---	---	✓	✓	✓
	952.8	TAG(58:6)	✓	---	---	✓	✓	✓

For TAG species, different neutral loss scans for identification of fatty acids were used and in most cases >3 fatty acids were identified. Thus, a single peak in the full MS scan is an overlay of different isobaric TAG species. There are no class specific scans for TAG species, so they were identified from the full MS scan. In the m/z area of 790 to

890 an overlay of PC and TAG species can occur. PC species are unambiguously identified by a NL scan for the PC headgroup. In addition a MS/MS spectrum of all signals above m/z of 790 was recorded. Compared to PC species, MS/MS spectra of TAG species show very intensive signals due to loss of fatty acids. Thus, MS/MS spectra were used to identify TAG species and resolve the possibility of an overlay with PC species, which show a characteristic signal at m/z 184.1. Lipids marked with an (^{L}) were detected with Liquid Extraction Surface Analysis (LESA) in positive ion mode with NL or PI scans (phospholipids and CEs) or in the full MS mode (TAG). Lipids marked with an asterisk (*) were previously identified with DESI-MS.[3]

Supplement Table IV: Lipids identified in endarterectomies (P1-3) and radial control arteries (C1-3) in negative MS mode.

	m/z [Ion]	Lipid	P1	P2	P3	C1	C2	C3
SM	709.7 [M-Cl]$^-$	SM(d18:1/14:0)*	✓	---	✓	---	---	---
	723.8 [M-Cl]$^-$	SM(d18:1/15:0)*	✓	✓	---	---	---	---
	733.4 [M-Ac]$^-$	SM(d18:1/14:0)*	✓	✓	✓	---	---	---
	735.6 [M-Cl]$^-$	SM(d18:1/16:1)*	✓	✓	---	---	---	---
	737.4 [M-Cl]$^-$	SM(d18:1/16:0)*	✓	✓	✓	---	✓	---
	739.5 [M-Cl]$^-$	SM(d18:0/16:0)	✓	✓	✓	---	---	---
	747.5 [M-Ac]$^-$	SM(d18:1/15:0)*	✓	✓	✓	---	---	---
	749.5 [M-Ac]$^-$	SM(d18:0/15:0)*	✓	✓	✓	---	----	---
	759.5 [M-Ac]$^-$	SM(d18:1/16:1)*	✓	✓	✓	---	✓	---
	761.5 [M-Ac]$^-$	SM(d18:1/16:0)*	✓	✓	✓	✓	✓	✓
	763.5 [M-Ac]$^-$	SM(d18:0/16:0)	✓	✓	✓	---	✓	✓
	789.5 [M-Ac]$^-$	SM(d18:1/18:0)*	✓	✓	---	---	✓	---
	795.7 [M-Cl]$^-$	SM(d18:0/20:0)	✓	✓	---	---	---	---
	843.5 [M-Cl]$^-$	SM(d18:1/24:3)	✓	✓	---	---	✓	---
	845.7 [M-Cl]$^-$	SM(d18:1/24:2)*	✓	✓	✓	---	---	---
	847.5 [M-Cl]$^-$	SM(d18:1/24:1)	✓	---	✓	---	---	---
	869.6 [M-Ac]$^-$	SM(d18:1/24:2)*	✓	✓	✓	---	---	---
	871.6 [M-Ac]$^-$	SM(d18:1/24:1)*	✓	✓	✓	---	✓	---
	873.6 [M-Cl]$^-$	SM(d18:1/24:0)	✓	✓	✓	---	---	---
IPC	530.3	IPC(16:0)*	✓	✓	---	---	---	---
	554.2	IPC(18:2)*	✓	---	✓	---	---	---
PC	792.4	PC(34:2)	✓	✓	---	---	--	---
	816.8	PC(36:4)	✓	✓	---	---	---	---
	818.7	PC(36:3)	✓	✓	---	---	---	---
	820.8	PC(36:2)	✓	✓	---	---	---	---
	822.7	PC(36:1)	✓	✓	✓	---	---	---
	848.1	PC(38:2)	✓	✓	✓	---	---	---
	850.0	PC(38:1)	✓	✓	---	---	---	---
PS	788.8	PS(36:1)	✓	✓	✓	✓	✓	✓
	810.8	PS(38:4)	✓	---	✓	✓	✓	---

812.8	PS(38:3)	✓	---	---	---	✓	---
816.8	PS(38:1)	---	---	---	---	✓	---
834.8	PS(40:6)	✓	---	---	✓	---	---
836.8	PS(40:5)	✓	✓	✓	---	✓	---
838.8	PS(40:4)	✓	---	✓	✓	✓	---

Lipids marked with an asterisk (*) were previously identified with DESI-MS.[3]

Supplement Table V: Quantitation of CE, SM, IPC and PC species in endarterectomies and radial arteries.

	Lipid species	Endarterectomies (n = 3)	Radial Arteries (n = 3)
CE	CE(10:0)	0.03 (±0.031)	0.00 (±0.000)
	CE(14:0)	0.08 (±0.024)	0.00 (±0.001)
	CE(16:0)	1.34 (±0.380)	0.01 (±0.004)
	CE(16:1)	1.09 (±0.199)	0.00 (±0.003)
	CE(18:0)	1.00 (±0.998)	0.01 (±0.005)
	CE(18:1)	8.75 (±1.017)	0.00 (±0.003)
	CE(18:2)	13.05 (±1.203)	0.01 (±0.004)
	CE(18:3)	0.65 (±0.159)	0.00 (±0.001)
	CE (20:0)	1.91 (±1.118)	0.07 (±0.046)
	CE(20:1)	0.86 (±0.305)	0.03 (±0.013)
	CE(20:2)	0.29 (±0.224)	0.03 (±0.015)
	CE(20:3)	1.31 (±0.447)	0.02 (±0.012)
	CE(20:4)	3.00 (±0.475)	0.07 (±0.036)
	CE(20:5)	0.79 (±0.273)	0.05 (±0.024)
	CE(22:3)	0.14 (±0.082)	0.00 (±0.000)
	CE(22:4)	0.20 (±0.131)	0.00 (±0.001)
	CE(22:5)	0.33 (±0.115)	0.00 (±0.000)
	CE(22:6)	0.58 (±0.202)	0.00 (±0.002)
∑		**35.40**	**0.30**
SM	SM(d18:1/14:0)	198.0 (±84.198)	6.61 (±1.123)
	SM(d18:1/15:0)	106.2 (±42.053)	2.81 (±0.428)
	SM(d18:1/16:1)	245.8 (±101.061)	13.7 (±2.211)
	SM(d18:1/16:0)	2381.2 (±815.959)	130.2 (±18.218)
	SM(d18:0/16:0)	0.0 (±0.000)	16.2 (±4.525)
	SM(d18:1/18:0)	194.9 (±50.536)	22.0 (±1.215)
	SM(d18:1/24:2)	576.3 (±232.9)	48.3 (±7.032)
	SM(d18:1/24:1)	1000.0 (±357.210)	75.4 (±18.375)
	SM(d18:1/24:0)	779.6 (±237.968)	46.2 (±6.921)
∑		**5482.0**	**361.4**
IPC	IPC(14:0)	0.3 (±0.186)	0.08 (±0.084)
	IPC(O-16:1)	0.4 (±0.180)	0.03 (±0.028)

	IPC(O-16:0)	3.2 (±2.224)	0.0 (±0.000)
	IPC(16:1)	6.4 (±3.787)	0.2 (±0.173)
	IPC(16:0)	226.2 (±82.92)	3.4 (±1.114)
	IPC(O-18:0)	10.7 (±4.468)	3.1 (±0.586)
	IPC(18:2)	79.7 (±52.028)	1.4 (±0.190)
	IPC(18:1)	125.0 (±67.418)	1.5 (±0.283)
	IPC(18:0)	139.4 (±45.472)	4.3 (±0.944)
	IPC(20:4)	39.6 (±18.225)	8.7 (±6.140)
	IPC(20:3)	23.1 (±11.614)	2.8 (±1.498)
	IPC(20:2)	6.8 (±2.875)	3.3 (±0.603)
	IPC(22:6)	0.0 (±0.000)	0.3 (±0.260)
	IPC(22:5)	0.2 (±0.214)	0.5 (±0.347)
	IPC(22:4)	2.2 (±2.230)	0.4 (±0.400)
	IPC(22:0)	0.0 (±0.000)	0.6 (±0.629)
	IPC(24:6)	0.0 (±0.000)	0.3 (±0.327)
	IPC(24:0)	0.0 (±0.000)	1.2 (±1.196)
∑		**663.5**	**33.5**
PC	PC(24:0)	0.0 (±0.000)	0.6 (±0.612)
	PC(26:0)	7.5 (±7.537)	30.0 (±15.883)
	PC(32:1)	145.8 (±35.995)	31.3. (±6.251)
	PC(32:0)	338.8. (±143.356)	67.3 (±8.742)
	PC(O-34:1)	86.7 (±29.938)	11.0 (±2.505)
	PC(34:2)	347.9 (±84.022)	71.5 (±22.006)
	PC(34:1)	574.0 (±167.714)	155.7 (±31.683)
	PC(O-36:5)	118.1 (±23.325)	49.2 (±24.949)
	PC(O-36:4)	99.0 (±29.058)	23.3 (±1.205)
	PC(36:4)	202.0 (±48.470)	71.4 (±18.798)
	PC(36:3)	230.1 (±66.385)	40.0 (±11.058)
	PC(36:2)	461.5 (±117.019)	70.0 (±16.422)
	PC(36:1)	485.5 (±122.935)	67.1 (±11.761)
	PC(O-38:5)	95.7 (±31.416)	18.8 (±8.375)
	PC(O-38:4)	70.9 (±21.676)	13.5 (±6.486)
	PC(38:6)	64.9 (±15.026)	15.6 (±7.430)
	PC(38:5)	83.7 (±25.984)	26.0 (±8.381)
	PC(38:4)	319.6 (±90.744)	65.4 (±18.571)
	PC(38:3)	459.4 (±135.207)	46.0 (±9.378)

PC(38:2)	567.1 (±177.947)	26.7 (±14.090)
PC(40:6)	33.6 (±10.728)	7.4 (±2.613)
PC(40:5)	26.4 (±12.732)	5.4 (±1.980)
PC(40:4)	30.8 (±10.157)	4.3 (±1.627)
PC(43:6)	1.8 (±1.089)	0.7 (±0.128)
PC(44:12)	4.8 (±0.952)	0.7 (±0.198)
PC(44:10)	0.3 (±0.283)	0.0 (±0.000)
∑	**4855.6**	**927.7**

Data are given in pmol/μL (mean ± SE) for CE or fmol/μL (mean ± SE) for lPC, PC and SM.

Supplement Table VI: Clinical characteristics of symptomatic and asymptomatic patients.

	Symptomatology	Age	Gender	DM	COPD	HTN	Renal failure	b-blockers	ASA	ACEI	Statins
Patient 4	Symptomatic	71	Male	No	No	Yes	No	No	Yes	Yes	No
Patient 5	Symptomatic	76	Male	Yes	No	Yes	No	No	Yes	Yes	Yes
Patient 6	Symptomatic	71	Male	No	No	Yes	Yes	No	Yes	Yes	Yes
Patient 7	Asymptomatic	62	Male	Yes	No	Yes	No	No	Yes	Yes	Yes
Patient 8	Asymptomatic	70	Male	No	No	Yes	No	No	Yes	Yes	Yes
Patient 9	Asymptomatic	71	Male	No	No	Yes	No	No	Yes	Yes	Yes
Patient 10	Symptomatic	84	Female	No	No	Yes	No	No	Yes	Yes	Yes
Patient 11	Symptomatic	78	Female	No	No	Yes	No	No	Yes	Yes	No
Patient 12	Symptomatic	71	Female	No	No	Yes	No	No	Yes	Yes	Yes
Patient 13	Asymptomatic	80	Female	No	No	Yes	No	No	Yes	Yes	Yes
Patient 14	Asymptomatic	65	Female	No	Yes	Yes	No	No	Yes	No	Yes
Patient 15	Asymptomatic	69	Female	Yes	No	Yes	No	No	Yes	Yes	Yes

For abbreviations, see footnote to Supplemental Table II.

Supplemental Table VII: Clinical characteristics of plaques divided in ruptured (unstable) and non-ruptured (stable) areas.

	Symptomatology	Age	Gender	DM	COPD	HTN	Renal failure	b-blockers	ACEI	Statins
Patient 16	Symptomatic	81	Male	No	No	Yes	No	No	No	Yes
Patient 17	Asymptomatic	70	Male	Yes	Yes	Yes	No	Yes	Yes	Yes
Patient 18	Symptomatic	54	Male	Yes	No	Yes	No	No	Yes	Yes
Patient 19	Symptomatic	76	Male	No	Yes	Yes	No	No	No	Yes
Patient 20	Symptomatic	79	Female	Yes	No	Yes	No	Yes	No	Yes
Patient 21	Symptomatic	73	Male	No	No	No	No	No	No	Yes (4 days)
Patient 22	Symptomatic	81	Male	No	No	Yes	No	Yes	Yes	Yes
Patient 23	Symptomatic	80	Female	Yes	No	Yes	Yes	No	No	Yes

For abbreviations, see footnote to Supplemental Table II.

Supplemental Table VIII: Quantitation of CE, SM, IPC and PC species in stable and unstable areas of the same plaques.

	Stable (n = 8)	Unstable (n = 8)	P value* (paired t-test)
CE species			
CE(10:0)	0.1 (±0.025)	0.2 (±0.083)	0.283
CE(14:0)	0.3 (±0.031)	0.5 (±0.174)	0.425
CE(16:0)	6.2 (±0.190)	6.3 (±0.284)	0.857
CE(16:1)	2.4 (±0.187)	2.8 (±0.393)	0.189
CE(18:0)	0.0 (±0.000)	2.1 (±0.799)	**0.036**
CE(18:1)	29.2 (±1.247)	26.3 (±1.885)	0.154
CE(18:2)	27.8 (±1.745)	31.2 (±1.655)	0.147
CE(18:3)	1.4 (±0.095)	1.7 (±0.242)	0.145
CE(20:0)	2.2 (±0.458)	3.7 (±0.589)	0.058
CE(20:1)	2.1 (±0.508)	2.2 (±0.117)	0.789
CE(20:2)	1.9 (±0.311)	1.9 (±0.345)	0.991
CE(20:3)	6.7 (±0.777)	3.6 (±0.345)	**0.006**
CE(20:4)	9.4 (±0.850)	8.5 (±0.960)	0.325
CE(20:5)	3.3 (±0.302)	3.5 (±0.343)	0.617
CE(22:3)	0.8 (±0.171)	0.8 (±0.359)	0.974
CE(22:4)	1.5 (±0.311)	0.8 (±0.175)	0.053
CE(22:5)	1.9 (±0.325)	1.8 (±0.236)	0.525
CE(22:6)	2.7 (±0.404)	2.2 (±0.425)	0.262
SM species			
SM(d18:0/16:0)	3.6 (±1.399)	3.2 (±1.839)	0.827
SM(d18:1/24:0)	11.6 (±2.180)	13.1 (±2.110)	0.687
SM(d18:1/24:1)	18.9 (±1.199)	20.9 (±1.451)	0.330
SM(d18:1/24:2)	14.0 (±1.602)	12.6 (±0.632)	0.371
SM(d18:1/14:0)	3.2 (±0.277)	3.5 (±0.316)	0.680
SM(d18:1/15:0)	1.2 (±0.111)	1.6 (±0.174)	**0.033**
SM(d18:1/16:0)	39.9 (±2.273)	38.0 (±2.407)	0.548
SM(d18:1/16:1)	4.0 (±0.414)	3.8 (±0.203)	0.612
SM(d18:1/18:0)	3.4 (±0.209)	3.3 (±0.216)	0.678
IPC species			

lPC(O-16:0)	0.1 (±0.064)	0.2 (±0.140)	0.171
lPC(16:0)	36.1 (±1.870)	35.2 (±1.994)	0.688
lPC(16:1)	0.2 (±0.099)	0.1 (±0.046)	0.180
lPC(O-18:0)	0.8 (±0.250)	1.3 (±0.284)	0.171
lPC(18:0)	22.3 (±1.674)	27.0 (±1.001)	**0.026**
lPC(18:1)	17.3 (±1.661)	12.1 (±1.852)	0.132
lPC(18:2)	10.1 (±0.967)	10.5 (±1.071)	0.650
lPC(20:2)	1.0 (±0.417)	2.5 (±0.713)	**0.029**
lPC(20:3)	2.8 (±0.478)	3.1 (±0.579)	0.626
lPC(20:4)	4.3 (±0.556)	4.7 (±0.848)	0.691
lPC(22:0)	0.1 (±0.056)	0.1 (±0.047)	0.540
lPC(22:4)	3.9 (±2.002)	1.9 (±1.041)	0.295
lPC(22:5)	0.3 (±0.193)	0.5 (±0.182)	0.365
lPC(22:6)	0.6 (±0.304)	0.8 (±0.318)	0.805
lPC(24:6)	0.1 (±0.110)	0.1(±0.093)	0.940
PC species			
PC(26:0)	0.2 (±0.062)	0.6 (±0.244)	0.081
PC(32:0)	5.3 (±0.365)	4.5 (±0.252)	0.193
PC(32:1)	2.2 (±0.216)	2.8 (±0.171)	**0.018**
PC(O-34:1)	1.8 (±0.214)	1.8 (±0.173)	0.942
PC(34:1)	15.2 (±0.824)	12.1 (±1.122)	**0.004**
PC(34:2)	8.3 (±0.829)	8.7 (±0.792)	0.645
PC(O-36:4)	2.0 (±0.286)	2.4 (±0.208)	0.375
PC(36:1)	5.7 (±1.169)	7.1 (±0.750)	0.331
PC(36:2)	9.4 (±0.485)	10.3 (±0.382)	0.204
PC(36:3)	5.8 (±0.241)	5.9 (±0.344)	0.791
PC(36:4)	7.5 (±0.518)	5.6 (±0.385)	**0.047**
PC(O-36:4)	2.9 (±0.598)	2.5 (±0.289)	0.570
PC(O-38:4)	1.5 (±0.276)	1.5 (±0.301)	0.993
PC(O-38:5)	2.6 (±0.333)	2.6 (±0.226)	0.960
PC(38:2)	5.2 (±1.222)	7.4 (±2.104)	0.336
PC(38:3)	6.6 (±0.990)	7.5 (±1.317)	0.621
PC(38:4)	8.8 (±0.405)	7.3 (±0.224)	**0.019**
PC(38:5)	3.0 (±0.162)	2.7 (±0.187)	0.308
PC(38:6)	2.1 (±0.346)	3.1 (±0.350)	0.060
PC(40:4)	1.0 (±0.084)	0.7 (±0.147)	0.063

PC(40:5)	1.0 (±0.197)	1.1 (±0.159)	0.731
PC(40:6)	1.7 (±0.099)	1.5 (±0.213)	0.285
PC(43:6)	0.1 (±0.023)	0.1 (±0.032)	0.344
PC(44:12)	0.1 (±0.022)	0.1 (±0.035)	**0.039**

Data presented are given in % (mean ± SE) for each single lipid class. * P-values were derived from paired Student's t-tests since stable and unstable areas were from the same plaque, bold numbers highlight p-values <0.05.

Supplemental Table IX: Clinical characteristics of patients with endarterectomies. The plasma of the patients were extracted with chloroform/methanol and analyzed with shotgun lipidomics.

	Plasma (n = 35)
Demographic	
Age, years (mean±SD)	69.0 (± 8.8)
Male, %	71.4
BMI, kg/m^2	25.4
Medical history, %	
DM	20.0
COPD	8.6
HTN	71.4
Renal failure	5.7
Medication	
b-blockers	22.9
ASA	71.4
ACEI	40.0
Statins	97.1

For abbreviations, see footnote to Supplemental Table II.

Supplemental Table X: Relative amount of CE, SM, IPC and PC species in human plasma and human atherosclerotic plaques.

	Plasma (n = 35)	Plaques (n = 28)	P value* (unpaired t-test)
CE species			
CE(10:0)	0.0 (±0.000)	0.1 (±0.026)	**<0.001**
CE(14:0)	0.3 (±0.016)	0.4 (±0.051)	**0.015**
CE(16:0)	6.9 (±0.167)	6.6 (±0.176)	0.209
CE(16:1)	2.6 (±0.199)	2.6 (±0.163)	0.769
CE(18:0)	0.0 (±0.000)	1.0 (±0.329)	**0.001**
CE(18:1)	30.0 (±0.446)	26.9 (±0.847)	**0.001**
CE(18:2)	41.4 (±0.766)	29.7 (±1.032)	**<0.001**
CE(18:3)	1.9 (±0.174)	1.4 (±0.100)	**0.026**
CE(20:0)	0.5 (±0.054)	4.5 (±0.556)	**<0.001**
CE(20:1)	0.0 (±0.000)	2.9 (±0.294)	**<0.001**
CE(20:2)	0.0 (±0.000)	1.8 (±0.210)	**<0.001**
CE(20:3)	0.0 (±0.000)	4.6 (±0.390)	**<0.001**
CE(20:4)	12.6 (±0.738)	8.5 (±0.482)	**<0.001**
CE(20:5)	2.5 (±0.235)	3.6 (±0.250)	**0.002**
CE(22:3)	0.0 (±0.000)	0.7 (±0.115)	**<0.001**
CE(22:4)	0.0 (±0.000)	0.9 (±0.131)	**<0.001**
CE(22:5)	0.0 (±0.000)	1.6 (±0.163)	**<0.001**
CE(22:6)	1.3 (±0.081)	2.2 (±0.185)	**<0.001**
SM species			
SM(d18:0/16:0)	1.6 (±0.182)	2.8 (±0.773)	0.107
SM(d18:1/14:0)	1.2 (±0.057)	3.6 (±0.184)	**<0.001**
SM(d18:1/15:0)	0.5 (±0.037)	1.4 (±0.091)	**<0.001**
SM(d18:1/16:1)	2.0 (±0.079)	4.2 (±0.174)	**<0.001**
SM(d18:1/16:0)	13.2 (±0.381)	43.1 (±1.675)	**<0.001**
SM(d18:1/18:0)	5.2 (±0.167)	3.3 (±0.182)	**<0.001**
SM(d18:1/24:2)	41.8 (±0.704)	11.8 (±0.683)	**<0.001**
SM(d18:1/24:1)	23.3 (±0.410)	19.0 (±0.753)	**<0.001**
SM(d18:1/24:0)	11.3 (±0.480)	10.8 (±1.146)	0.681
IPC species			

IPC(O-16:0)	0.0 (±0.000)	0.1 (±0.045)	**0.041**
IPC(16:0)	40.7 (±0.803)	36.5 (±1318)	**0.006**
IPC(16:1)	0.5 (±0.087)	0.1 (±0.033)	**<0.001**
IPC(O-18:0)	0.0 (±0.000)	1.1 (±0.162)	**<0.001**
IPC(18:0)	13.3 (±0.317)	24.6 (±1.094)	**<0.001**
IPC(18:1)	14.9 (±0.411)	14.5 (±1.179)	0.708
IPC(18:2)	17.2 (±0.611)	9.4 (±0.629)	**<0.001**
IPC(20:2)	0.0 (±0.000)	2.2 (±0.551)	**<0.001**
IPC(20:3)	2.4 (±0.180)	3.2 (±0.489)	0.080
IPC(20:4)	8.1 (±0.363)	5.7 (±0.962)	**0.015**
IPC(22:0)	0.0 (±0.000)	0.1 (±0.028)	**0.011**
IPC(22:4)	0.0 (±0.000)	1.7 (±0.688)	**0.008**
IPC(22:5)	0.0 (±0.000)	0.3 (±0.083)	**0.001**
IPC(22:6)	0.8 (±0.121)	0.5 (±0.139)	0.142
IPC(24:6)	0.0 (±0.000)	0.1 (±0.041)	**0.044**
PC species			
PC(26:0)	0.0 (±0.000)	0.7 (±0.264)	**0.004**
PC(O-32:0)	0.1 (±0.005)	0.0 (±0.000)	**<0.001**
PC(O-32:1)	0.1 (±0.005)	0.0 (±0.000)	**<0.001**
PC(32:0)	0.7 (±0.017)	6.0 (±0.476)	**<0.001**
PC(32:1)	0.9 (±0.048)	2.7 (±0.210)	**<0.001**
PC(32:2)	0.3 (±0.007)	0.0 (±0.000)	**<0.001**
PC(O-34:1)	0.4 (±0.013)	1.8 (±0.111)	**<0.001**
PC(O-34:2)	0.3 (±0.012)	0.0 (±0.000)	**<0.001**
PC(O-34:3)	0.2 (±0.009)	0.0 (±0.000)	**<0.001**
PC(34:1)	11.8 (±0.329)	15.0 (±0.711)	**<0.001**
PC(34:2)	15.4 (±0.407)	8.6 (±0.408)	**<0.001**
PC(34:3)	0.6 (±0.031)	0.0 (±0.000)	**<0.001**
PC(35:4)	0.0 (±0.000)	2.1 (±0.157)	**<0.001**
PC(36:1)	5.2 (±0.258)	6.3 (±0.523)	0.051
PC(36:2)	10.0 (±0.209)	10.0 (±0.250)	0.920
PC(36:3)	7.4 (±0.170)	5.5 (±0.153)	**<0.001**
PC(36:4)	11.9 (±0.367)	6.1 (±0.385)	**<0.001**
PC(36:5)	2.2 (±0.151)	0.0 (±0.000)	**<0.001**
PC(O-36:4)	0.0 (±0.000)	2.8 (±0.288)	**<0.001**
PC(O-38:4)	1.4 (±0.032)	1.3 (±0.142)	0.642

PC(O-38:5)	1.7 (±0.030)	2.2 (±0.168)	**<0.001**
PC(38:2)	2.0 (±0.090)	5.9 (±0.947)	**<0.001**
PC(38:3)	3.7 (±0.098)	7.2 (±0.652)	**<0.001**
PC(38:4)	7.9 (±0.287)	7.6 (±0.309)	0.372
PC(38:5)	4.5 (±0.106)	2.5 (±0.133)	**<0.001**
PC(38:6)	5.8 (±0.262)	2.4 (±0.172)	**<0.001**
PC(O-40:5)	0.5 (±0.018)	0.0 (±0.000)	**<0.001**
PC(O-40:6)	0.8 (±0.029)	0.0 (±0.000)	**<0.001**
PC(40:4)	0.4 (±0.017)	0.8 (±0.067)	**<0.001**
PC(40:5)	1.0 (±0.046)	0.9 (±0.100)	0.453
PC(40:6)	2.1 (±0.096)	1.4 (±0.115)	**<0.001**
PC(41:5)	0.1 (±0.004)	0.0 (±0.000)	**<0.001**
PC(41:6)	0.1 (±0.005)	0.0 (±0.000)	**<0.001**
PC(43:6)	0.0 (±0.004)	0.1 (±0.023)	0.090
PC(44:12)	0.1 (±0.005)	0.1 (±0.025)	0.411

Data presented are given in % (mean ± SE) for each single lipid class. * P-values were derived from unpaired Student's t-tests, bold numbers highlight p-values <0.05.

Supplemental Figure I

A

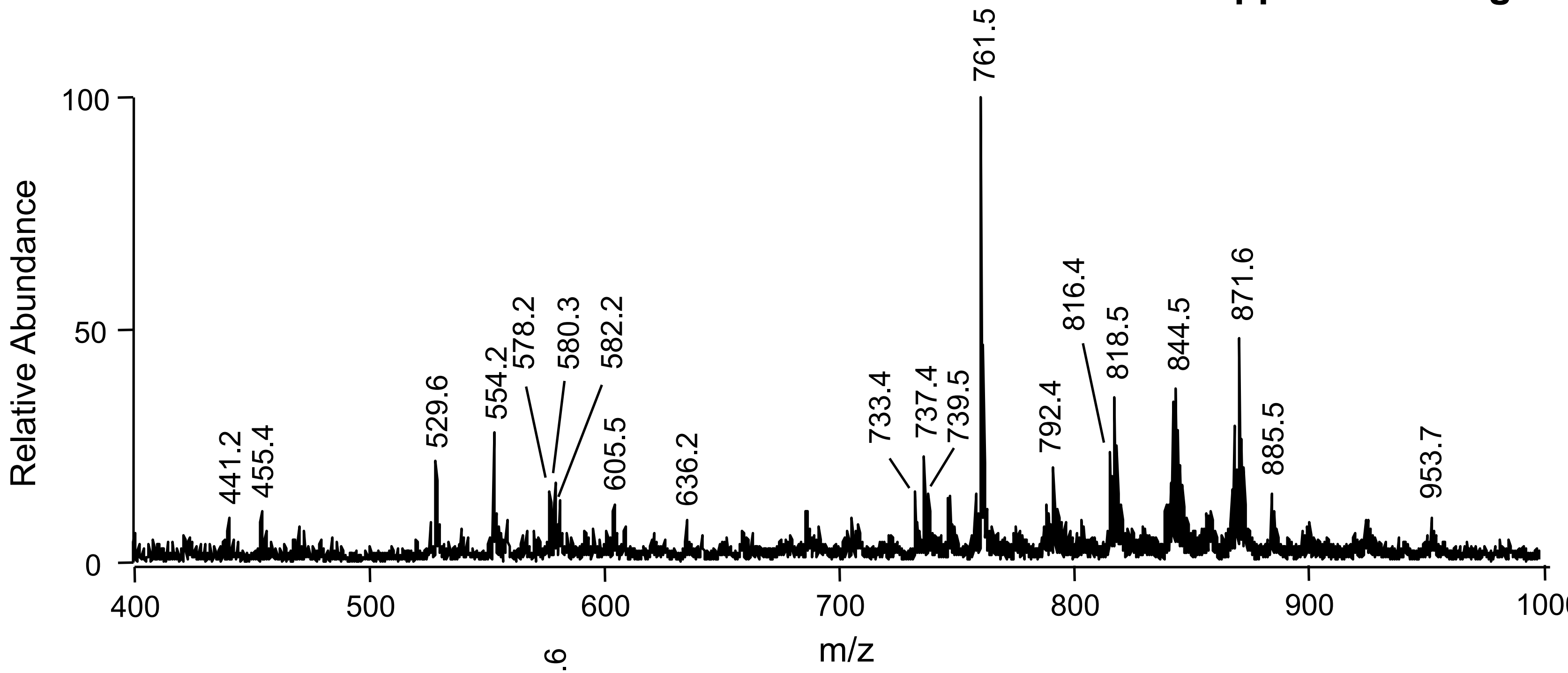

B

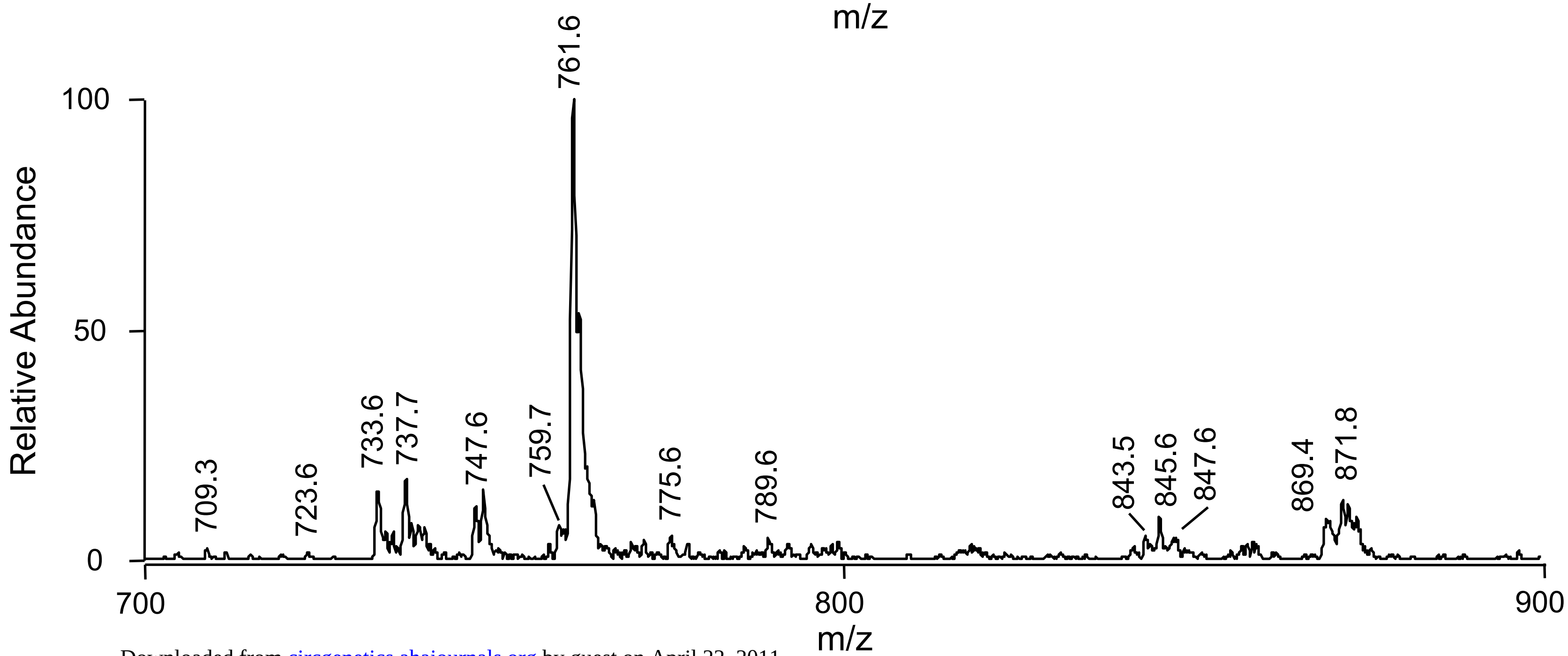

Supplemental Figure II

Symptomatic versus asymptomatic plaques

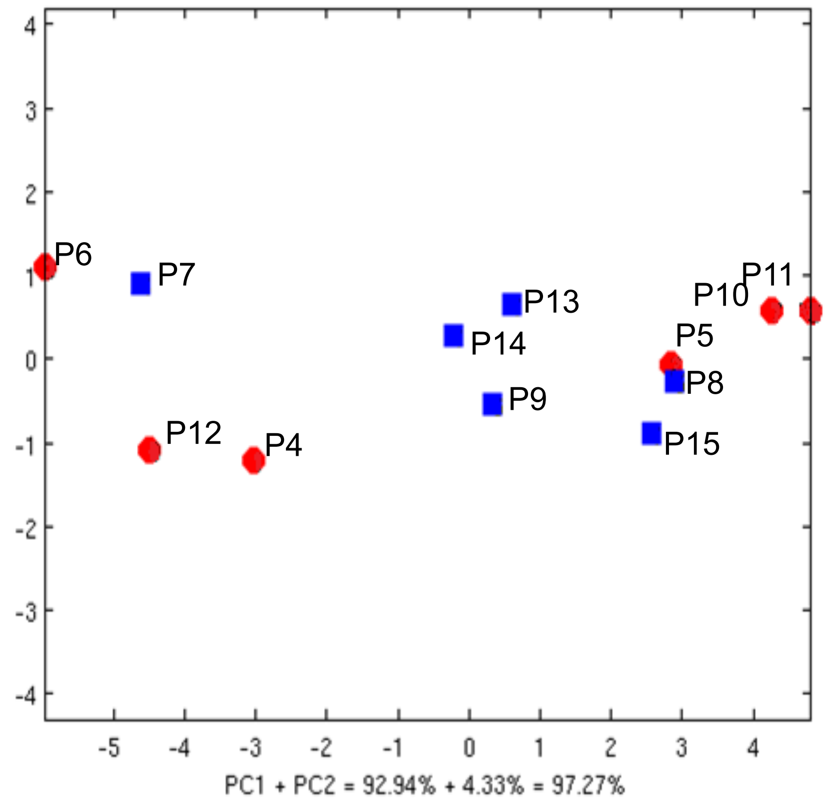

Magnitude of 2 first PCs (all measurements)

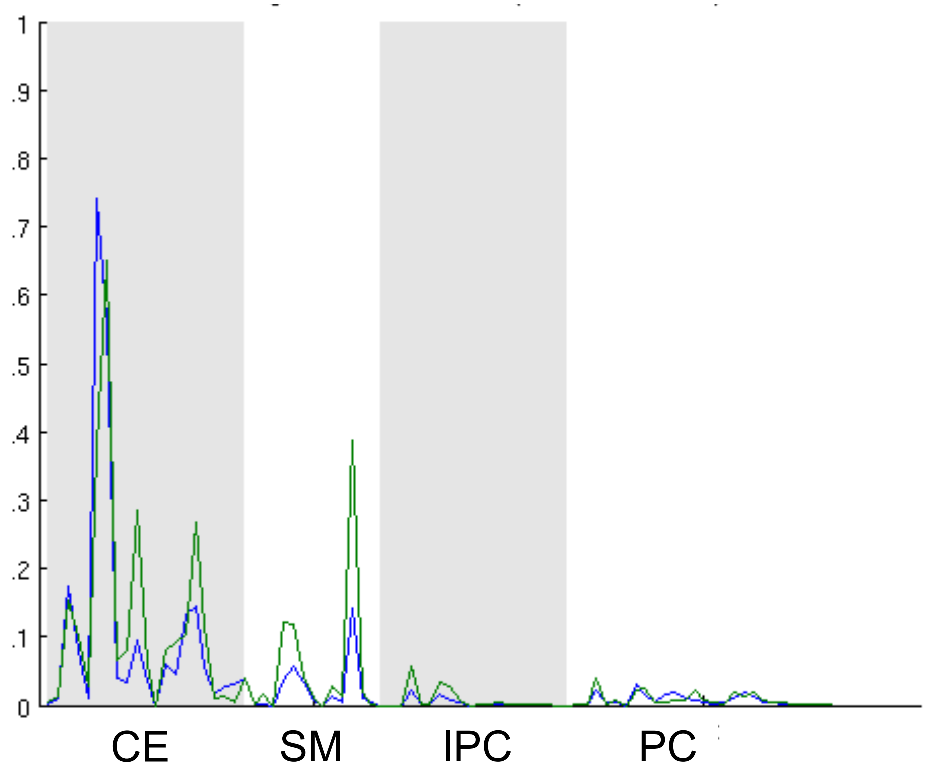

Supplemental Figure III

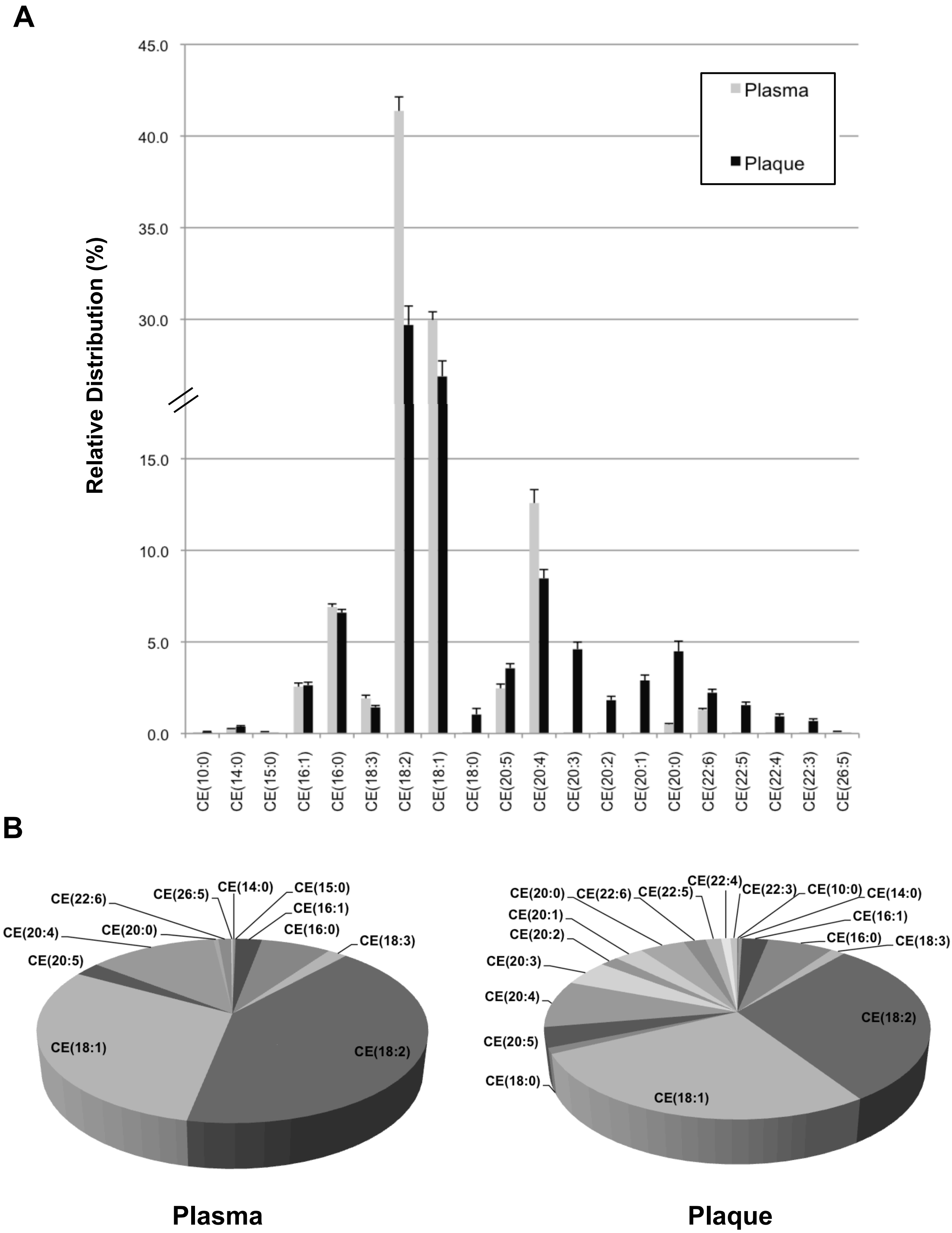

Supplemental Figure IV

A

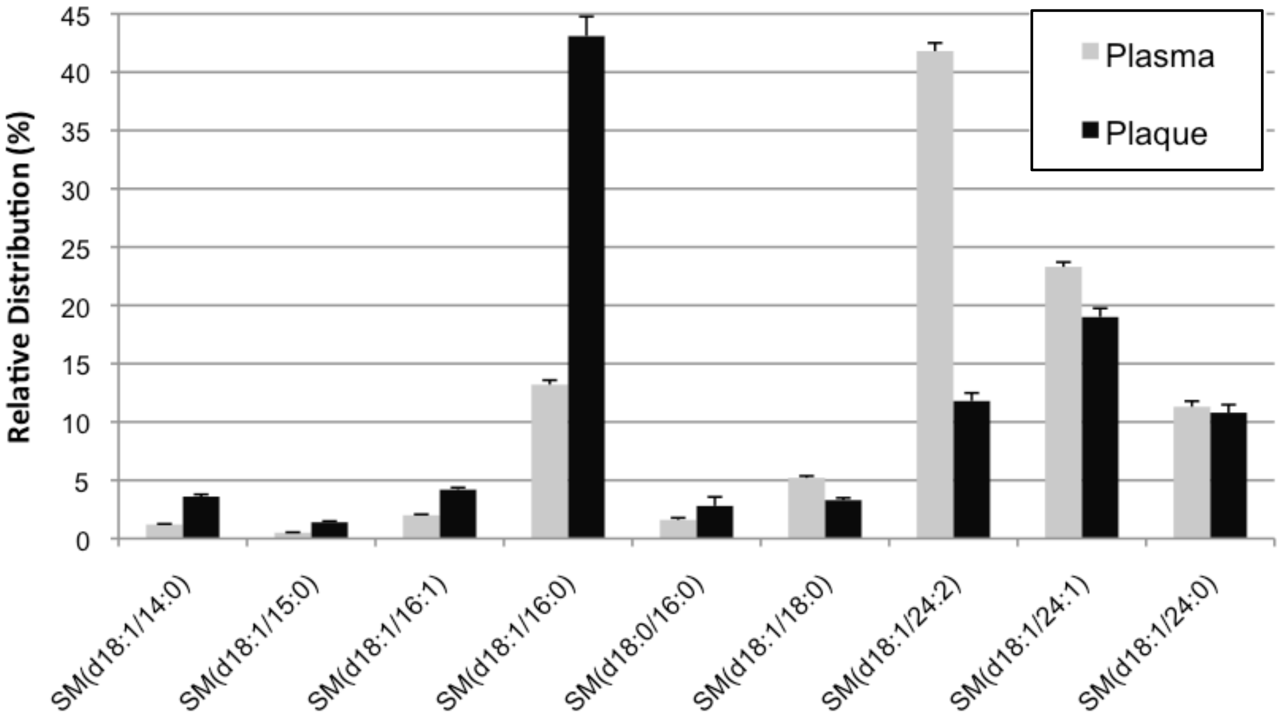

B

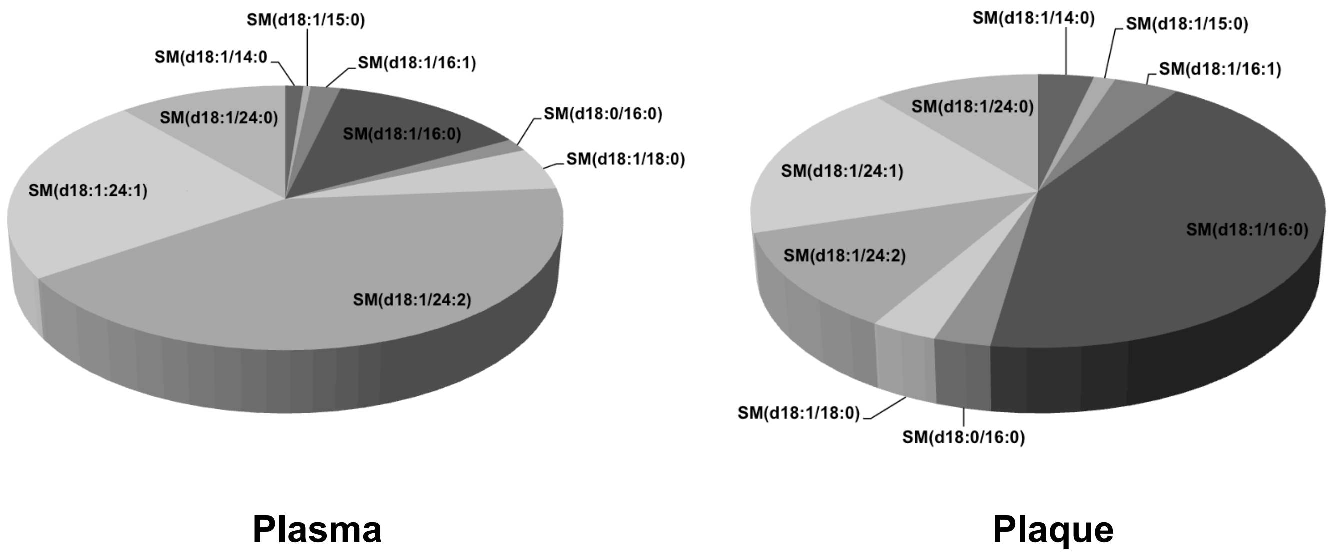

Supplemental Figure V

A

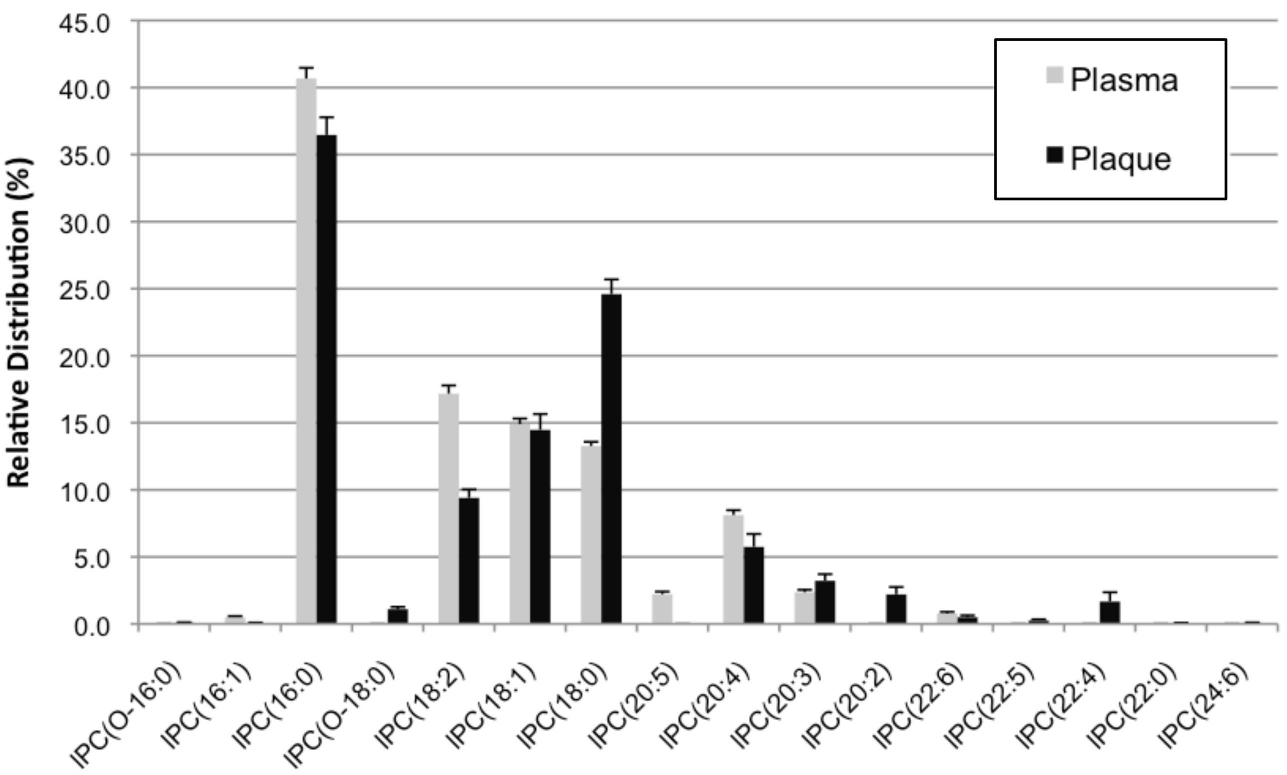

B

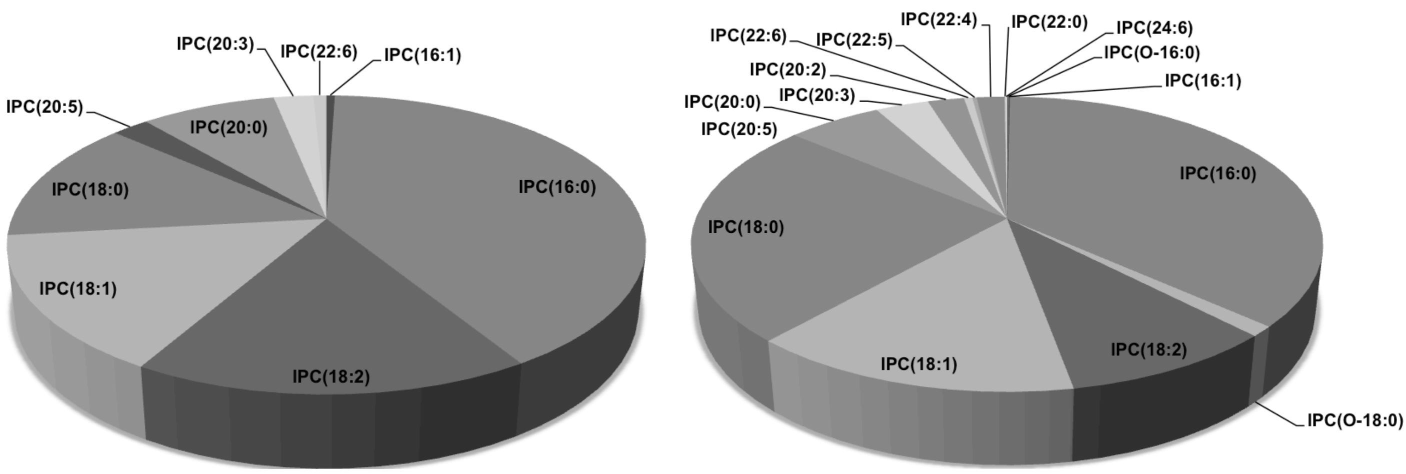

Plasma

Plaque

Supplemental Figure VI